Paper citation:
Douglas S. Auld, Scott Lovell, Natasha Thorne, Wendy A. Lea, David J. Maloney, Min Shen, Ganesha Rai, Kevin Battaile, Craig J. Thomas, Anton Simeonov, Robert P. Hanzlik, and James Inglese, "Molecular Basis for the High Affinity Binding and Stabilization of Firefly Luciferase by PTC124." Proc. Nat. Acad. Sci. USA 2010, 107, 4878-83. PMID 20194791

Keywords:
Ataluren, multi-substrate adduct inhibitor, X-ray crystallography, protein stability

Abstract:
Firefly luciferase (FLuc), an ATP-dependent bioluminescent reporter enzyme, is broadly used in chemical biology and drug discovery assays. PTC124 (Ataluren; **1**; (3-[5-(2-fluorophenyl)-1,2,4-oxadiazol-3-yl]benzoic acid), unique in its *m*aryl carboxylate moiety and discovered in an FLuc-based assay targeting nonsense codon suppression, is an unusually potent FLuc-inhibitor. Paradoxically, PTC124 and related analogs increase cellular FLuc activity levels by post-translational stabilization. In this study, we show that FLuc inhibition and stabilization is the result of an inhibitory product formed during the FLuc-catalyzed reaction between its natural substrate, ATP, and PTC124. A 2.0 Å co-crystal structure revealed the inhibitor to be the acyl-AMP mixed-anhydride adduct PTC124-AMP, which was subsequently synthesized and shown to be a high-affinity multisubstrate adduct inhibitor (MAI; KD = 120pM) of FLuc. Biochemical assays, LC-MS, and near-attack conformer modeling demonstrate that formation of this novel MAI is absolutely dependent upon the precise positioning and reactivity of a key *meta*-carboxylate of PTC124 within the FLuc active site. We also demonstrate that the inhibitory activity of PTC124-AMP is relieved by free Coenzyme A, a component present at high concentrations in luciferase detection reagents used for cell-based assays. This explains why PTC124 can appear to increase, instead of inhibit, FLuc activity in cell-based reporter gene assays. To our knowledge, this is the first example in which the "off-target" effect of a small molecule is mediated by an MAI mechanism.

Text of paper:

Douglas S. Auld, Scott Lovell, Natasha Thorne, Wendy A. Lea, David J. Maloney, Min Shen, Ganesha Rai, Kevin Battaile, Craig J. Thomas, Anton Simeonov, Robert P. Hanzlik, and James Inglese, "Molecular Basis for the High Affinity Binding and Stabilization of Firefly Luciferase by PTC124." Proc. Nat. Acad. Sci. USA 2010, 107, 4878-83. PMID 20194791. Publisher's official version: http://dx.doi.org/10.1073/pnas.0909141107

Molecular Basis for the High Affinity Binding and Stabilization of Firefly Luciferase by PTC124

Douglas S. Auld[a], Scott Lovell[b], Natasha Thorne[a], Wendy A. Lea[a], David J. Maloney[a], Min Shen[a], Ganesha Rai[a], Kevin Battaile[c], Craig J. Thomas[a], Anton Simeonov[a], Robert P. Hanzlik[b], and James Inglese [a, 1]

[a]NIH Chemical Genomics Center, National Institutes of Health, Bethesda, MD 20892-3370, USA.

[b]Structural Biology Center, University of Kansas, 2121 Simons Drive, Lawrence, KS 66047.

[c]IMCA-CAT, Advanced Photon Source, Argonne National Laboratory, 9700 South Cass Avenue, Bldg 435A**,** Argonne, IL 60439

[1]To whom correspondence should be addressed. E-mail: jinglese@mail.nih.gov, Phone: 301- 217-5733, Fax: 301-217-5736

Classification: Biological Science, Biochemistry

Key words: Ataluren, multi-substrate adduct inhibitor, X-ray crystallography, protein stability.

Approximate length: (text and figures): 36,999 characters. Four Figures. Supplemental Information and figure files also provided.

Abbreviations: CRCs, concentration-response curves; MAI, multisubstrate adduct inhibitor; FLuc, firefly (*Photinus pyralis*) luciferase; $FLuc^{UGA}$, FLuc gene with UGA codon at position 190; DLSA, 5'-O-[N-(dehydroluciferyl)-sulfamoyl]adenosine; LH_2, luciferin; L, dehydroluciferin; L-AMP, dehydroluciferyl-AMP; NAC, near-attack conformer; sa-Ade, acylsulfamide adenosine

Douglas S. Auld, Scott Lovell, Natasha Thorne, Wendy A. Lea, David J. Maloney, Min Shen, Ganesha Rai, Kevin Battaile, Craig J. Thomas, Anton Simeonov, Robert P. Hanzlik, and James Inglese, "Molecular Basis for the High Affinity Binding and Stabilization of Firefly Luciferase by PTC124." Proc. Nat. Acad. Sci. USA 2010, 107, 4878-83. PMID 20194791. Publisher's official version: http://dx.doi.org/10.1073/pnas.0909141107

\body

Introduction

Firefly luciferase from *Photinus pyralis* (FLuc) is an ATP-dependent luciferase widely used as a reporter enzyme for cell-based gene expression assays, principally due to the high sensitivity and large dynamic range bioluminescence affords (1, 2). However, as an enzyme that catalyzes the bimolecular reaction between two small molecule substrates, D-luciferin and ATP, it is prone to inhibition by a variety of low-molecular weight heterocyclic compounds typically found in screening collections (3, 4). Expressed intracellularly as a reporter, the FLuc enzyme has a short protein half-life ($t_{½}$ ~3 hrs) relative to other reporters (5, 6). While ideal for following dynamic responses in cell-based assays, reporter instability can be offset by ligand-induced stabilization. Stabilization of FLuc by compounds acting as inhibitors can lead to a relative increase in enzyme levels (compared to untreated basal levels), and correspondingly increased FLuc activity—a counterintuitive result for compounds characterized as FLuc inhibitors (5-8).

We have previously shown that PTC124, a compound with putative nonsense codon suppression activity (9) (Ataluren™; **1**, Table 1), and related 3,5-diaryl oxadiazoles, are FLuc inhibitors that stabilize the enzyme intracellularly, leading to a transcriptional- and translational-independent increase in the observed enzyme activity over basal levels (7, 8). Past efforts to profile the NIH Molecular Libraries Small Molecule Repository (MLSMR) for compounds that inhibit FLuc originally identified MLS000062114 (**2**; PubChem CID: 2876651 Table 1) —a molecule equivalent to the *des*-carboxylate analog of PTC124— as a FLuc inhibitor (3). While **2** showed low

micromolar potency in our profile study (3, 8), we observed that introduction of a *m*-carboxylate at R_2 (i.e., PTC124; **1**) resulted in a significantly more potent FLuc inhibitor (IC_{50} ~10 nM) (8). Paradoxically, we also found that PTC124 caused an *activation* response in FLuc cell-based reporter gene assays, including those expressing FLuc from a wild-type *luc*+ gene, with typical compound incubation times (16-24 hrs) indicative of potent enzyme stabilization (8) by PTC124.

Ligand-receptor affinity arises from alignment of shape and electrostatic features between receptor and ligand (10). On rare occasions, the unique arrangement of these elements can lead to enzymatically-assisted formation of an even higher affinity multisubstrate adduct inhibitor (MAI). By combining components of both substrates into a single molecule, the resulting conjugate gains a large entropic advantage, and its affinity can often be estimated by the product of the substrate K_Ds (11). The ligation of two substrates with micromolar affinity can thus result in an MAI with potency in the sub-nanomolar range (12). In recent years, this principle has been used in the domain of fragment-based ligand design (13). While the majority of MAI's described in the literature have been prepared synthetically (14), precedence exists for MAI generation by the target enzyme itself (15, 16). An FLuc-generated MAI – the mixed anhydride dehydroluciferyl-AMP (L-AMP) - is naturally formed by the oxidation of luciferyl-AMP (LH_2-AMP), an intermediate in the conversion of D-luciferin to oxyluciferin (17, 18) (Fig. 1A; see Supporting Information (*SI*) *Appendix*, Fig. S1A). The L-AMP MAI acts as a potent inhibitor of FLuc, with an IC_{50} = 6 nM (K_D = 500 pM) (17). The enzyme-catalyzed production of an MAI from PTC124 and ATP could explain the exceptional affinity of PTC124 against FLuc in both enzyme and cell-based assays.

With this study, we describe the mechanism of formation, high affinity binding and stabilization of FLuc by PTC124. The X-ray co-crystal structure of FLuc bound to PTC124 and the substrate ATP revealed the presence of an enzyme-bound PTC124-AMP mixed-anhydride (**6**) analogous to the L-AMP intermediate in the FLuc catalytic reaction. PTC124 binds to the luciferin pocket allowing the reaction of the *m*-carboxylate of PTC124 with ATP yielding the mixed anhydride PTC124-AMP —an MAI for which we measured a K_D of 120 pM. Using a series of 3,5-diaryl oxadiazole analogs containing nonreactive carboxyl biosteres we demonstrate that formation of the MAI critically depends on the aryl *m*-carboxylate moiety of PTC124. Formation of this MAI and its association with the enzyme ultimately results in potent enzyme inhibition, dramatic thermal stabilization of FLuc, and the paradoxical increase in FLuc activity observed in cell-based assays with PTC124. The MAI mechanism for PTC124 was not anticipated because classical MAIs are based on substrate analogs (19) and the 3,5-diaryl oxadiazole core is not a luciferin analog. This represents the first time a synthetic compound has been shown to mediate "off-target" effects by an MAI mechanism. Further, and seemingly contradictory, is the ability of the apparent MAI-bound FLuc reporter activity to be fully measured in bioluminescent endpoint assays. This is possible because the MAI bound to FLuc is sensitive to FLuc-mediated thiolysis by free Coenzyme A (CoASH), a component of most FLuc detection reagents. The findings presented here provide essential guidance for the use of luciferase assays in chemical biology and drug discovery efforts, while more specifically identifying the mechanism of action of PTC124 in FLuc cell-based assays.

Results

Crystal structures. The structure of an apo form of luciferase (Luc:apo; PDB: 3IEP) was determined to 2.1Å resolution by molecular replacement (see Methods and *SI Appendix*, Table S1; Fig S2). Apo crystals were soaked in the presence of PTC124 (**1**, *SI Appendix*, Table 1) and ATP and the resulting co-cyrstal structure (PDB: 3IES) electron density maps were examined for ligand binding. Surprisingly, clear density was observed for an adduct of AMP with PTC124 (PTC124-AMP; **6**, Table 1 and Fig. 1A,B), apparently resulting from nucleophilic displacement of pyrophosphate from ATP by the *m*-carboxylate of PTC124 (*SI Appendix*, Fig. S1B). The AMP portion of **6** forms hydrogen bonds with luciferase residues (Fig. 1C) and the diaryl oxadiazole group is positioned in a hydrophobic pocket near Ala 348 and Ile 351 and shows aromatic stacking with Phe 247 (Fig. 2A,B). Therefore, PTC124-AMP fully occupies the active site of FLuc (Fig. 1D). The PTC124-AMP structure was found to make critical H-bonds with several invariant residues including Asp 422, which is within H-bonding distance to the 2'-OH of the ribose ring (Fig. 2A,B) (20).

The binding mode of this inhibitor is similar to that observed for ligand-bound Japanese firefly (*Luciola cruciata*) luciferase (LcrLuc) (21). Alignment of our FLuc co-crystal structure and the structure of LcrLuc co-crystallized with the L-AMP analog 5'-O-[N-(dehydroluciferyl)-sulfamoyl] adenosine (DLSA) (PDB: 2D1S)(21, 22) shows that PTC124-AMP binds with the 3,5-diaryl oxadiazole within the luciferin pocket with the *m*-carboxylate specifically located to form the mixed anhydride with AMP (Fig. 3 A, B) in a manner that is iso-structural with DLSA (Fig. 2C; *SI Appendix*, Fig. S3A). The planar nature of the 3,5-diaryl oxadiazole provides for an orientation in the active site similar to the natural substrate D-luciferin and positions the carboxylate to fulfill a rare case of

enzyme inhibition wherein the enzyme catalyzes the formation of its own inhibitor. This represents the first time an intermediate of the luciferase reaction coordinate has been trapped crystallographically. Remarkably, PTC124-AMP represents a structural mimicry of the luciferyl-AMP intermediate (LH_2-AMP; Fig. 1A and *SI Appendix*, Fig. S1A) that gives rise to luminescence via dioxetanone formation, and to formation of the naturally-occurring potent inhibitor of the enzyme, L-AMP via a side reaction (18) (Fig. 1A and *SI Appendix*, Fig. S1A).

The structure of FLuc:PTC124-AMP is quite similar overall to the apo structure with an overall RMSD of 0.60 Å between Cα atoms (*SI Appendix*, Fig. S3B). The largest structural difference is present in the loop between Ser 314 and Leu 319, which moves to accommodate ligand binding (Fig. 2D). This loop shows well-defined electron density in the ligand-bound form and has a similar conformation to the homologous loop of LcrLuc bound to DLSA.

Solution formation of the MAI by FLuc. LC-MS was used to confirm the FLuc-dependent synthesis of PTC124-AMP in solution. Incubation of PTC124 and ATP alone did not yield any mass corresponding to PTC124-AMP, with only the parent compound peak of PTC124 observed (*SI Appendix*, Fig. S4A). Addition of FLuc to the same sample resulted in loss of the parent compound peak and appearance of the PTC124-AMP mass (*SI Appendix*, Fig. S4A). Additionally, the yield of PTC124-AMP obtained could be titrated by varying the FLuc concentration (*SI Appendix*, Fig. S4B). The lack of reaction in the absence of FLuc is expected due to the high energy required for the negatively charged carboxylate group to come into van der Waals contact with the triphosphate moiety of ATP, as well as the necessary desolvation of the carboxylate

water shell. However, in the active site of the enzyme, the correct 'near attack conformers' (NACs) of the reactants are brought within van der Waals distance allowing bond formation, presumably via S_N2 displacement (Fig. 3A) (23).

The *meta*-carboxylate provides the optimal NAC. To further understand the reactivity of the *m*-carboxylate, we modeled the *ortho*-, *meta*-, and *para*-carboxylate regioisomers of PTC124 (i.e. compounds **10, 6** and **7**, respectively) into the crystal structure (Fig. 3B). This showed that reaction with ATP requires the *p*-isomer (**7**) to rotate approximately 20˚ in-plane away from the position in which *m*-isomer (**1**) binds (Fig. 3B). This is somewhat unfavorable energetically, as indicated by the decreased potency of *p*-isomer (**7**) as an inhibitor (Table 1). However, formation of the MAI from *o*-PTC124 (**10**) would require complete rotation out of the luciferin binding pocket, suggesting that this NAC could not be achieved in the FLuc active site (Fig. 3B, **10**; *SI Appendix*, Fig. S3C). Consistent with these models, using equivalent incubation times (~ 10 min) and high FLuc concentrations (20 μM), we were able to detect the presence of *p*-PTC124-AMP at an intermediate level upon incubation of **7** with FLuc and ATP (Fig. 3C,D). However, when we incubated **10** with FLuc and ATP under the same conditions, we did not observe any conversion and no product corresponding to *o*-PTC124-AMP was observed (Fig. 3C,D).

Potency depends on the aryl *m*-carboxylate. To further investigate the effect of the *m*-carboxylate on potency, we synthesized several carboxylate R_2 regioisomers and nonreactive analogs (Table 1) and determined their IC_{50}s against purified FLuc using [S] ~ K_M (e.g. both ATP and D-luciferin were at concentrations near their K_Ms so that the

observed IC_{50} approximated the true inhibitor affinity, K_I). Varying the *meta* substituent to either an amide (**3**) or the tetrazole (**4**) carboxylate biostere resulted in >100-fold loss in potency against the enzyme (Table 1). The *des*-carboxylate analog of PTC124 (**2**) demonstrated 80-fold lower potency, suggesting that *meta* substitution can add little toward the binding energy in the absence of adduct formation. Significantly, the potency of the synthetic PTC124-AMP (**6**) was approximately the same as that determined with PTC124 in the presence of ATP and FLuc, consistent with solution formation of adduct. Additionally, we measured the competition of synthetically prepared LH_2-AMP from FLuc by PTC124-AMP and PTC124 (in the absence of ATP). From these data we were able to estimate a K_D = 120±30 pM for PTC124-AMP and 1.4 ±0.4 μM for PTC124 using the method described by Rhodes et al (*SI Appendix*, Fig. S5) (17). Therefore, the K_D of PTC124 for FLuc improves by ~10,000-fold upon acyl-phosphoryl anhydride MAI formation.

We previously noted a decrease in potency for *p*-carboxylate analogs (8), which is confirmed here. In agreement with this series being less competent to form the PTC124-AMP MAI, we observed smaller shifts in potency between *p*-carboxylate and non-reactive derivatives. Changing the *p*-carboxylate substituent to either an amide (**8**) or tetrazole (**9**) resulted in potency shifts of ~ 10-fold (Table 1), significantly less than those observed between the *m*-carboxylate analogs (**1, 3, 4**). Again in line with our previously determined pharmacological correlation between potency in the FLuc enzyme assay and the cell-based FLuc nonsense codon suppression assay (8) – both PTC124 (**1**) and the *m*-carboxylate analog (**5**) demonstrated potent (< 100 nM) activity in either assay, while the *p*-carboxylate analog of PTC24 (**7)** demonstrated weak (μM)

potency in these assays. As well, we found that *ortho*-carboxylate analogs (**10, 11**) demonstrated the greatest reduction in potency in both assays (Table 1).

In an effort to investigate further the potency differences between the *meta* and *para* carboxylate analogs, we prepared stable analogs of the *meta* and *para* adducts (**12, 13**; Table 1). These were prepared as acylsulfamide derivatives, so as to limit any possibility of hydrolysis influencing the potency measurement. We found that both stable adducts (**12** and **13**) showed potent inhibition similar to anhydride **6** (Table 1). Further, when we pre-incubated the *p*-carboxylate analog (**7**) or PTC124 with ATP and FLuc (10 nM) in the enzyme assay we observed no time-dependent increase in inhibition by either compound (IC_{50} = 4±3 nM without pre-incubation and 4±0.6 nM with a 24 hr pre-incubation for PTC124; for **7**, IC_{50} = 1.1±0.3 μM and 3.8±0.3 μM for the respective conditions). Therefore, under these enzymological conditions (i.e., low FLuc concentrations) formation of *p*-PTC124-AMP is kinetically unfavorable. Thus, given the near equal inhibition potencies for the pre-made adduct analogs (**6**, **12**, and **13**) we conclude that the much weaker inhibition potency observed for **7** is due to a kinetic effect. This is further supported by the NAC models, with the potency governed by the rates of formation and breakdown of the adduct.

FLuc thermal stabilization parallels inhibitor potency. To further probe the interaction of FLuc with PTC124 and its analogs, we used a fluorescence-based thermal denaturation assay designed to assess the stabilization of proteins by small molecules (24). The melting curves for FLuc in the presence of varying concentrations of PTC124 showed a maximum ΔT_m = 8 °C (at 200 μM concentration), while inclusion of 2 mM ATP in the buffer significantly enhanced this by 4.6 °C (*SI Appendix*, Fig. S6). Overall, the

ΔT_m shifts of FLuc in the presence of compound correlated well with the potency of the compound against the enzyme. The most dramatic enhancement in FLuc stabilization occurred in the presence of either PTC124 or an analog in which the *m*-carboxylate was preserved (ΔT_m = 12-13 °C in the presence of ATP; Fig. 4A; **1, 5**). This was followed closely by the *p*-carboxylate analog of PTC124 (**7**). On the other hand, the *m*-substituted analogs containing moieties incapable of adduct formation, such as the *m*-amide (**3**) or *m*-tetrazole (**4**) displayed much lower ΔT_m enhancements in the presence of ATP. Not surprisingly, the lowest ΔT_m values were obtained for the *o*-carboxylate (**10**) and *o*-amide (**11**) analogs. Significantly, we also found a very large enhancement in thermal stability of FLuc in the presence of synthetically prepared PTC124-AMP (**6**), which showed a ΔT_m = 28 °C (Fig. 4B; *SI Appendix*, Fig. S6C,D**)**. The large ΔT_m observed for synthetically prepared PTC124-AMP lends further support to the MAI stabilization hypothesis.

MAI formation explains FLuc cell-based activity. To examine if PTC124 and analogs increased luciferase enzyme activity in cells in a manner consistent with protein stabilization by MAI formation, compounds were tested in a cell-based assay similar to that used to discover PTC124 ($FLuc^{UGA}$) (9). This assay employs cells expressing FLuc from a cDNA with a nonsense mutation at codon 190 of the FLuc gene ($pFLuc190^{UGA}$) (8). Although a nonsense mutation in the coding region is present in the FLuc mRNA produced in these cells, preventing efficient translation of full length protein, there is still an extremely low, but detectable, basal level of FLuc activity due to sporadic translational readthrough of the nonsense mutation (25). When cells expressing $pFLuc190^{UGA}$ were treated with compound, we again found that PTC124 (**1**) showed the

most potent activation, followed by the *p*- and *o*-carboxylate analogs (**7** and **10**), respectively, which follows the same trend established by thermal denaturation experiments and enzyme inhibition data (Fig. 4C**;** *SI Appendix*, Fig. S7A). Efficacy in the cell-based assay was similar for both the *m*- and *p*-carboxylate analogs (**1**, **7**; $FLuc^{UGA}$ % Activation in Table 1 and see *SI Appendix*, Fig. S7A) suggesting that intracellulary, a stabilized enzyme-inhibitor complex is also formed with these compounds, although the concentration at which this is achieved varies. However, the *o*-carboxylate (**10**), which is not predicted to form the MAI, demonstrates significantly reduced activation in the cell-based assay (Table 1) with only partial CRCs (*SI Appendix*, Fig. S7A). Shifts in cell-based activation for regioisomers and analogs correlated well with enzymatic inhibitory potency (Fig. 4D), as an example, both the *p*-carboxylate (**7**) and the *m*-tetrazole (**4**) analogs displayed reduced potency in both assays (~100-fold less potent). Further, as expected from the NAC analysis, the potency of the *o*-carboxylate (**10**) and *o*-amide (**11**) were relatively weak in both the enzyme and cell-based assays. The only inconsistency seen between the cell-based and biochemical assay was for the *des*-carboxylate analog (**2**), which, though still supporting the critical nature of the *m*-carboxylate, displayed weaker activity in the cell based assay (EC_{50} ~10 μM) than in the purified FLuc enzyme assay (IC_{50} ~ 1 μM; Table 1). This might reflect poor cell-permeability of the compound due to serum binding or poor solubility in the cell media, ultimately resulting in decreased potency for this compound in the cell-based assay. Overall, however, potency in the cell-based assay followed the order of reactivity of the compound in forming the MAI, that is, the carboxylate reactivity of *meta* > *para* >>*ortho*,

as predicted by the FLuc co-crystal structure and corresponding NAC models for the active site of FLuc.

CoASH effects on PTC124 potency. CoASH has been shown to significantly reduce FLuc inhibition by the L-AMP MAI via an enzymatically-catalyzed thiolytic reaction that converts L-AMP to L-CoA (see *SI Appendix*, Fig. S1) (18). CoASH is also a common constituent of detection reagents used for firefly luciferase assays, as it increases the bioluminescent signal through relief of L-AMP inhibition and thus provides more efficient use of the substrate D-luciferin (18). As PTC124 forms a potent PTC124-AMP MAI, we sought to determine if addition of CoASH to the FLuc enzyme reaction would also relieve PTC124-AMP MAI inhibition, potentially via the same mechanism demonstrated for L-AMP – thiolytic conversion of PTC124-AMP to PTC124-CoA (*SI Appendix*, Fig. S1). We found this to be the case with addition of 500 μM CoASH (a concentration likely equal to what is typically used in commercial detection reagents for cell-based assays) to purified FLuc enzyme assays reducing the potency of PTC124 (**1**) by approximately 35-fold, on average (*SI Appendix*, Fig. S7B-E; Table S2). The potency of the *p*-carboxylate analog (**7**) was reduced to a lesser degree (~10-fold), consistent with the reduced propensity for this analog to form the MAI. Consistent with thiolysis as the reason for reduced potency (versus a potential allosteric role for CoASH binding), we did not observe any shift in potency for the stable MAI analogs, **12** and **13**, in the presence of CoASH (IC_{50} remaining at 3±1 nM in either condition; *SI Appendix*, Fig. S7D,E; Table S2). Of note, addition of a higher concentration of cysteine (1 mM) did not affect the potency of PTC124 against FLuc (*SI Appendix,* Fig. S7B,C), indicating that

the reaction with CoASH is specific, and cannot be generalized to simple reducing reagents or nucleophiles (18).

Discussion

This study demonstrates that the molecular basis for high affinity binding of PTC124 to FLuc arises from the enzyme-catalyzed formation of an MAI through a key *m*-carboxylate group. The co-crystal structure is similar to that reported for LcrLuc bound to DLSA, a stable sulfamoyl analog of oxidized luciferin and AMP (21). The differential activity of 3,5-diaryl oxadiazole carboxylate regioisomers in FLuc cell-based assays can be explained by the crystal structure-supported NAC models. These models indicate that placement of the PTC124 carboxylate at the *ortho* or *para* position either prevents or impairs, respectively, alignment of the necessary functionalities needed for MAI formation. Experimentally, it was also found that FLuc-dependent formation of *ortho* and *para* carboxylate adducts was either nonexistent or proceeded with dramatically reduced efficiency. Further, the PTC124-AMP adduct formed either enzymatically, or by direct chemical synthesis, results in an inhibitor with nanomolar potency and high affinity binding to FLuc (K_D of ~100 pM).

Enhancement of protein stability through ligand-induced conformational changes or modulation of folding pathway equilibria is well-documented (26, 27), and can be reflected by increases in protein thermal stability. Thermal denaturation assays of FLuc in the presence of PTC124-AMP show a large ΔT_m of nearly 30 ºC, significantly greater than the sum of the ΔT_m values for PTC124 and ATP at the same concentration, suggesting that the formation of the adduct is essential for the observed increase in

protein stability. 3,5-diaryl oxadiazole analogs containing non-reactive acid isosteres at the *meta* position (**3-5**), and carboxylate-containing regioisomers at the *ortho* (**10**) or *para* (**7**) positions, also have significantly reduced thermal shifts, further indicating that FLuc protein stability is dependent on PTC124-AMP formation.

The apparent activity (or inactivity) of PTC124 in the cell-based assay depends on the assay protocol and the commercial detection reagent used (28, 29). As mammalian cells lack D-luciferin, intracellular binding of PTC124 to FLuc occurs without competing endogenous ligands. Cellular ATP saturates the FLuc nucleotide binding site, thus facilitating PTC124-AMP formation, high affinity binding, and both inhibition and stabilization of the enzyme. Detection of the associated increase in relative FLuc activity in cell-based assays can be readily achieved by wash-out of the inhibitor prior to detection, and/or addition of appropriate detection reagents containing excess substrates and co-factors (8, 9, 28, 29).

Catalysis of the ATP-dependent oxidation of D-luciferin to oxyluciferin, AMP, CO_2 and light involves an LH_2-AMP intermediate that can be oxidized to form an L-AMP by-product, a potent FLuc inhibitor (17, 18; *SI Appendix,* Fig. S1) . Commercially available FLuc detection reagents (e.g. BrightGlo™, Promega) contain high levels of CoASH that relieve FLuc inhibition by L-AMP via thiolysis, thereby optimizing FLuc luminescence (30). We show that addition of high micromolar concentrations of CoASH to the FLuc enzymatic assay significantly decreases the potency of PTC124 and *m*-carboxylate analogs. Conceivably, CoASH in detection reagents reacts with PTC124-AMP to create a PTC124-CoA adduct. The resulting shift in potency parallels that observed for the conversion of L-AMP (6 nM) to L-CoA (5 μM) (18). The application of commercial

detection mixes (which have relatively high concentrations of D-luciferin, ATP, and CoASH) will promote thiolysis and dissociation of the PTC124-AMP components from the enzyme, facilitating an interpretation of increased enzyme activity as apparent activation in the reporter gene assay.

It is not uncommon for a compound to demonstrate a higher potency when assayed against its isolated molecular target compared to that obtained for the target in a cellular context, as is seen for PTC124 (**1**), in which there is an ~10-fold decrease in potency for the cell-based assay (Table 1, compare IC_{50} and EC_{50}). One possible explanation for this could be due to competition by intracellular substrates or co-factors. Intracellular ATP, for example, could compete directly with PTC124-AMP association. Additionally, CoASH may thiolytically react with FLuc-bound PTC124-AMP to form the less potent PTC124-CoA, which is expected to stabilize the enzyme only at higher compound concentrations. However, it is likely that in an intracellular environment lacking D-luciferin, and in which PTC124 and saturating concentrations of ATP are present, enzymatic reformation of the high affinity MAI is favored. Therefore, the reduced potency observed in the $FLuc^{UGA}$ cell-based assay (~nM) relative to the measured K_D of the PTC124-AMP (~pM) against FLuc, and the fact that the cell-based structure-activity relationships parallel the catalytic requirements of FLuc for MAI formation, support the notion that enzymatic rounds of PTC124-AMP hydrolysis/reformation may occur in cells, the extent of which is dependent on the cellular quantity and availability of CoASH.

The prevalence of compounds that cause the paradoxical inhibitor-based-reporter stabilization in cell-based assays can be significant, reaching 20-60% of the

actives selected from cell-based FLuc assays aimed at activation (7). The counterintuitive nature of this phenomenon defies *post hoc* conventional wisdom and requires counter-screens designed to recognize compound-mediated reporter stabilization. One such example is an FLuc reporter system with attenuated expression (e.g. SV40 promoter) (31). This work highlights the importance of determining the potency of compounds active in cell-based FLuc assays against purified FLuc in the presence of defined concentrations of substrates ([S] ~ K_m) as opposed to using formulated detection reagents whose components can mask or alter inhibitory activity (7, 8, 28, 29). Finally, reporters with mechanistically distinct modes of bioluminescence such as RLuc can be used in orthogonal assays to confirm that compound activity is not biased by choice of reporter (8).

The original identification of PTC124 arose from a FLuc cell-based assay of nonsense codon suppression (9). To date, the only concentration-response data which suggests PTC124 is a nanomolar potent nonsense codon suppression agent has been derived solely from FLuc-based assays (9, 28). Divergence of the SAR associated with biochemical inhibition of FLuc and the cellular activation phenotype in FLuc-based nonsense codon suppression assays ($FLuc^{UGA}$) would argue for dual mechanisms of action for PTC124, supporting the existence of a cellular target mediating readthrough of premature termination codons. However, the dependence on the *m*-carboxylate functional group of PTC124 in the cell-based $FLuc^{UGA}$ assay was mirrored in the FLuc biochemical inhibition assay and thermal denaturation assay. The parallel nature of these responses is due to a rare and remarkable mechanism of enzyme inhibition – the formation of an MAI – and supports our previous observations that PTC124 activity is

reporter-dependent and nonsense codon-independent, increasing the activity of both $FLuc^{UGA}$ and wild type FLuc, respectively in cell-based assays while demonstrating inactivity in a corresponding $RLuc^{UGA}$ assay (8). Taken together, these results question the biological plausibility for a molecular target other than FLuc as the reason for increased cellular luciferase activity.

Methods

Crystallization of FLuc, X-ray data collection, and processing. All X-ray diffraction data were collected at the Advanced Photon Source (APS), IMCA-CAT beamline 17BM using an ADSC Quantum 210 CCD detector. Details of the crystallization are provided in the *SI* Methods and Table S1.

LC-MS. Compound (20 μM) and ATP (2 mM) in PBS were pre-mixed and further incubated with Fluc (20 μM or varied), or PBS as no-enzyme control, for 2 min at RT. Selective ion monitoring of the PTC124/analogs parent ion, the corresponding adduct, and the total ion current, was achieved on an Agilent 6130 Quadrupole MS detector. Additional information is in the *SI* Methods.

Molecular Modeling. FRED (OpenEye Scientific Software, Santa Fe, NM) docking was performed on the *para*- and *ortho*-PTC124-AMP adducts using a X-ray crystal structure of luciferase with PTC124-AMP bound. Full details are given in the *SI* Methods.

Thermal melt experiments. Using conditions described in the *SI* Methods, data was recorded on a iQ5 Real Time PCR Detection system (Bio-Rad) using a temperature range from 20 ºC to 95 °C in increments of 1 °C and a ramping rate of 0.1°C/s. Fluorescence intensity changes (Ex 490/Em 575 nm) were monitored with a charge-coupled device (CCD) camera. For more detail see *SI* Methods.

Determination of FLuc potencies. Potency was determined using a defined buffer with 10 μM of each substrate (ATP and D-luciferin) as previously described (8) using 10 nM *P. pyralis* luciferase (EC 1.13.12.7). Coenzyme A (C3019; Sigma) and DL-cysteine

(861677; Sigma) were added to the substrate reagent for specified experiments for final concentrations of 500 μM and 1 mM, respectively. Luminescence was detected using ViewLux (PerkinElmer).

Cell-based FLuc nonsense codon suppression assays: Grip-Tite 293 cells (Invitrogen) were transfected according to standard procedure (*SI* Methods) with a construct containing the reporter FLuc with a nonsense mutation at codon 190 (construct pFLuc190^{UGA} ; prepared by GenScript Corp.). In 1,536-well format, cells were seeded at 4,000 cells/well and compound was added one-hour post-seeding. 48 hours later cells were washed 3X with 1X PBS before detection mix was added to lyse cells and quantitate FLuc activity. Luminescence was detected using ViewLux (PerkinElmer). Additional detail is provided in *SI* Methods.

Chemical synthesis procedures. PTC124 (**1**) and analogs were prepared by methods similar to those previously described (8), and synthetic schemes and supporting analytical data are provided in *SI* Methods**.**

Accession codes. The structures have been deposited to the Protein Data Bank under the following accession codes (Luc:PTC124-AMP, PDB: 3IES; Luc:Apo, PDB: 3IEP ; Luc:Apo2, PDB: 3IER).

ACKNOWLEDGEMENTS. This research was supported by the Molecular Libraries Initiative of the NIH Roadmap for Medical Research, and an NIH COBRE award (5P20 RR17708) to the University of Kansas (KU). We thank Nadya Galeva from the KU Mass Spectrometry Laboratory for her assistance with the MALDI-MS analysis, and Bill Leister of the NCGC for analytical chemistry support.

References

1. Fan F & Wood KV (2007) Bioluminescent assays for high-throughput screening. *Assay Drug Dev Technol* 5(1):127-136.
2. Roda A, Guardigli M, Michelini E, & Mirasoli M (2009) Bioluminescence in analytical chemistry and *in vivo* imaging. *Trends in Analytical Chemistry* 28(3):307-322.
3. Auld DS*, et al.* (2008) Characterization of chemical libraries for luciferase inhibitory activity. *J Med Chem* 51(8):2372-2386.
4. Heitman LH*, et al.* (2008) False positives in a reporter gene assay: identification and synthesis of substituted N-pyridin-2-ylbenzamides as competitive inhibitors of firefly luciferase. *J Med Chem* 51(15):4724-4729.
5. Thompson JF*, et al.* (1997) Mutation of a protease-sensitive region in firefly luciferase alters light emission properties. *J Biol Chem* 272(30):18766-18771.
6. Thompson JF, Hayes LS, & Lloyd DB (1991) Modulation of firefly luciferase stability and impact on studies of gene regulation. *Gene* 103(2):171-177.
7. Auld DS, Thorne N, Nguyen DT, & Inglese J (2008) A specific mechanism for nonspecific activation in reporter-gene assays. *ACS Chem Biol* 3(8):463-470.
8. Auld DS, Thorne N, Maguire WF, & Inglese J (2009) Mechanism of PTC124 activity in cell-based luciferase assays of nonsense codon suppression. *Proc Natl Acad Sci U S A* 106(9):3585-3590.
9. Welch EM*, et al.* (2007) PTC124 targets genetic disorders caused by nonsense mutations. *Nature* 447(7140):87-91.

10. Fersht AR, *et al.* (1985) Hydrogen bonding and biological specificity analysed by protein engineering. *Nature* 314(6008):235-238.

11. Jencks WP (1975) Binding energy, specificity, and enzymic catalysis: the Circe effect. *Adv. Enzymol. Relat. Areas. Mol. Biol.* 43:219-410.

12. Inglese J, Blatchly RA, & Benkovic SJ (1989) A multisubstrate adduct inhibitor of a purine biosynthetic enzyme with a picomolar dissociation constant. *J Med Chem* 32(5):937-940.

13. Congreve M, Chessari G, Tisi D, & Woodhead AJ (2008) Recent developments in fragment-based drug discovery. *J Med Chem* 51(13):3661-3680.

14. Korolev S, *et al.* (2002) The crystal structure of spermidine synthase with a multisubstrate adduct inhibitor. *Nat Struct Biol* 9(1):27-31.

15. Inglese J & Benkovic SJ (1991) Multisubstrate Adduct Inhibitors of Glycinamide Ribonucleotide Transformylase: Synthesis and Enzyme-Assembled *Tetrahedron* 47(14/15):2351-2364.

16. Greasley SE, *et al.* (2001) Unexpected formation of an epoxide-derived multisubstrate adduct inhibitor on the active site of GAR transformylase. *Biochemistry* 40(45):13538-13547.

17. Rhodes WC & Mc EW (1958) The synthesis and function of luciferyl-adenylate and oxyluciferyl-adenylate. *J Biol Chem* 233(6):1528-1537.

18. Fraga H, Fernandes D, Fontes R, & Esteves da Silva JC (2005) Coenzyme A affects firefly luciferase luminescence because it acts as a substrate and not as an allosteric effector. *FEBS J* 272(20):5206-5216.

19. Broom AD (1989) Rational design of enzyme inhibitors: multisubstrate analogue inhibitors. *J Med Chem* 32(1):2-7.

20. Conti E, Lloyd LF, Akins J, Franks NP, & Brick P (1996) Crystallization and preliminary diffraction studies of firefly luciferase from *Photinus pyralis*. *Acta crystallographica* 52(Pt 4):876-878.

21. Nakatsu T*, et al.* (2006) Structural basis for the spectral difference in luciferase bioluminescence. *Nature* 440(7082):372-376.

22. Branchini BR, Murtiashaw MH, Carmody JN, Mygatt EE, & Southworth TL (2005) Synthesis of an N-acyl sulfamate analog of luciferyl-AMP: a stable and potent inhibitor of firefly luciferase. *Bioorg Med Chem Lett* 15(17):3860-3864.

23. Hur S, Kahn K, & Bruice TC (2003) Comparison of formation of reactive conformers for the S_N2 displacements by CH_3CO_2- in water and by Asp124-CO_2- in a haloalkane dehalogenase. *Proc Natl Acad Sci U S A* 100(5):2215-2219.

24. Ericsson UB, Hallberg BM, Detitta GT, Dekker N, & Nordlund P (2006) Thermofluor-based high-throughput stability optimization of proteins for structural studies. *Anal Biochem* 357(2):289-298.

25. Parker J (1989) Errors and alternatives in reading the universal genetic code. (*Microbiol Rev* 53(3):273-298.

26. Pace CN, Shirley BA, & Thomson JA (1989) *Measuring conformational stability of a protein in Protein Structure* (IRL Press, NY).

27. Thompson PA*, et al.* (2008) Identification of ligand binding by protein stabilization: comparison of ATLAS with biophysical and enzymatic methods. *Assay Drug Dev Technol* 6(1):69-81.

28. Peltz SW, *et al.* (2009) Nonsense suppression activity of PTC124 (Ataluren). *Proc Natl Acad Sci U S A* 106(25):E64.

29. Inglese J, Thorne N, & Auld DS (2009) Reply to Peltz et al: Post-translational stabilization of the firefly luciferase reporter by PTC124 (Ataluren). *PNAS* 106:E65.

30. Wood KV (1995) The chemical mechanism and evolutionary development of beetle bioluminescence. *Photochemistry and Photobiology* 62(4):662-673.

31. Lyssiotis CA, *et al.* (2009) Reprogramming of murine fibroblasts to induced pluripotent stem cells with chemical complementation of Klf4. *Proc Natl Acad Sci U S A* 106(22):8912-8917.

Douglas S. Auld, Scott Lovell, Natasha Thorne, Wendy A. Lea, David J. Maloney, Min Shen, Ganesha Rai, Kevin Battaile, Craig J. Thomas, Anton Simeonov, Robert P. Hanzlik, and James Inglese, "Molecular Basis for the High Affinity Binding and Stabilization of Firefly Luciferase by PTC124." Proc. Nat. Acad. Sci. USA 2010, 107, 4878-83. PMID 20194791. Publisher's official version: http://dx.doi.org/10.1073/pnas.0909141107

Table Captions:

Table 1. Potency and cellular activity of analogs in the enzymatic (FLuc) and cell-based (FLuc^{UGA}) assays. Potency of the compounds in the enzymatic and cell-based assays are given in μM. In the case of enzyme assays the values are averages ± the s.d. from at least three experimental replicates performed on different days and in the cell-based assay these values are averages ± the s. d. from at least two experimental replicates performed on different days. The enzyme assay was performed with FLuc at 10 nM and in the presence of 10 μM ATP and D-luciferin. Compounds that only partially inhibit (i.e. have reduced efficacy against) the FLuc enzyme are denoted by an asterisk next to their IC_{50} values. IC_{50} values estimated from CRCs with reduced efficacy generally are of lesser confidence. An experiment to test the potency of the adduct (**6**) in the cell-based assay (FLuc^{UGA}) was not conducted, due to stability and solubility issues of the adduct in DMSO, the solvent necessary to deliver compound to the cells. Adduct (**6**) was dissolved in PBS for enzyme assays (FLuc). sa-Ade, acylsulfamide adenosine.

Figure Captions

Figure 1. (**A**) Comparison of the structure of the mix anhydrides of AMP (left) with PTC124, D- luciferin (LH2), dehydroluciferin (L), and DLSA. (**B**) Fo-Fc omit map of the PTC124-AMP mixed anhydride contoured at 3σ. (**C**) Hydrogen-bonded interactions between PTC124-AMP MAI (**6**, ball and stick) and luciferase residue (sticks) are indicated as dashed lines. (**D**) Co-crystal X-ray structure of FLuc and PTC124-AMP MAI.

Figure 2: Substrate binding pocket of FLuc with PTC124-AMP bound (**A, B**). (**C**) Structure of FLuc (gray ribbon) liganded with PTC124-AMP (turquoise) overlaid on the structure of DLSA (gold) bound to LcrLuc (gray ribbon; PDB: 2D1S) showing the close similarity of ligand binding modes. Leu286 in FLuc corresponds to Ile288 in LcrLuc. These residues are located at the end of the respective ligand binding pockets, but whereas Ile288 moves upon ligand binding, Leu286 does not. (**D**) Overlay of the structures of apo-FLuc (magenta) and FLuc liganded with the PTC124-AMP MAI adduct (**6**, turquoise) showing movement of a loop between residues Ser314 and Leu319 upon binding of ligand (ball and stick).

Figure 3: NAC analysis of carboxylate PTC124 regioisomers. (**A**) Schematic of bond formation as the *m*-carboxylate of PTC124 displaces the pyrophosphate from ATP. (**B**) NAC modeling of PTC124/analogs within the FLuc active site. The *m*-carboxylate of PTC124 (**1**) provides an optimal NAC as the 3,5-diaryl oxadiazole is optimally positioned within the luciferin binding pocket. However, for the *p*-carboxylate analog (**7**), must rotate by ~20^{o} within the constraints of a productive NAC model to be able to form a NAC and react with ATP. For the *o*-carboxylate analog (**10**) to maintain

the NAC, a classic biaryl steric clash between the *o*-carboxylate and the adjacent oxadiazole occurs necessitating out of plane rotation which effectively pushes the analog out of the luciferin binding pocket, preventing MAI formation. (**C, D**) Graphs show formation of adenylate adducts by FLuc as analyzed by LC-MS. Total ion current (TIC) data for regioisomers of PTC124 mass (**C**), or the corresponding AMP adduct mass (**D**), following incubation of 20 μM PTC124 in the presence of 2 mM ATP for the regioisomers (indicated in **D**). Percentages represent the % remaining of the parent ion peak, calculated from the ratio of the peak areas for the compound incubated with ATP in the presence and absence of FLuc.

Figure 4. **Correlation between stabilization and inhibitor potency.** Compounds are identified in **Table 1.** (**A**) The stabilizing effect of PTC124 analogs, as demonstrated by ΔT_m,on 1.8 μM Fluc in the presence of 2 mM ATP correlates with their IC_{50}s for for FLuc inhibition *in vitro*. The maximum ΔT_m is plotted. Compounds showing decreasing ΔT_m also show lower inhibitor potency against the enzyme. (**B**) The ΔT_m values for PTC124 (**1**), PTC124 + 2 mM ATP, and the synthetically prepared PTC124-AMP adduct (**6**) are shown in either PBS (***i***) or Tris-acetate buffer (***ii***). The higher ΔT_m value obtained for the synthetic adduct is likely due to the fact that this adduct is measured in the absence of ATP (2 mM). Adding an equivalent concentration of ATP to **6** yielded the same ΔT_m value (12.6 °C) as was observed with PTC124 and ATP. (**C**) A correlation plot of the EC_{50} values in the cell-based FLuc nonsense codon suppression assay plotted against their IC_{50} values in the purified FLuc enzymatic assay for PTC124, a regioisomer, and related analogs. Inhibition of purified FLuc in an enzymatic assay follows the same trend as apparent activation in a cell-based FLuc reporter gene assay. (**D**) Fold-shift in

IC_{50} values for PTC124 analogs relative to PTC124 (**1**) in the FLuc enzyme assay (***i***) and the nonsense codon suppression cell-based assay (***ii***) indicate that the potency trends remain largely similar in both types of assay.

Douglas S. Auld, Scott Lovell, Natasha Thorne, Wendy A. Lea, David J. Maloney, Min Shen, Ganesha Rai, Kevin Battaile, Craig J. Thomas, Anton Simeonov, Robert P. Hanzlik, and James Inglese, "Molecular Basis for the High Affinity Binding and Stabilization of Firefly Luciferase by PTC124." Proc. Nat. Acad. Sci. USA 2010, 107, 4878-83. PMID 20194791. Publisher's official version: http://dx.doi.org/10.1073/pnas.0909141107

Figure 1

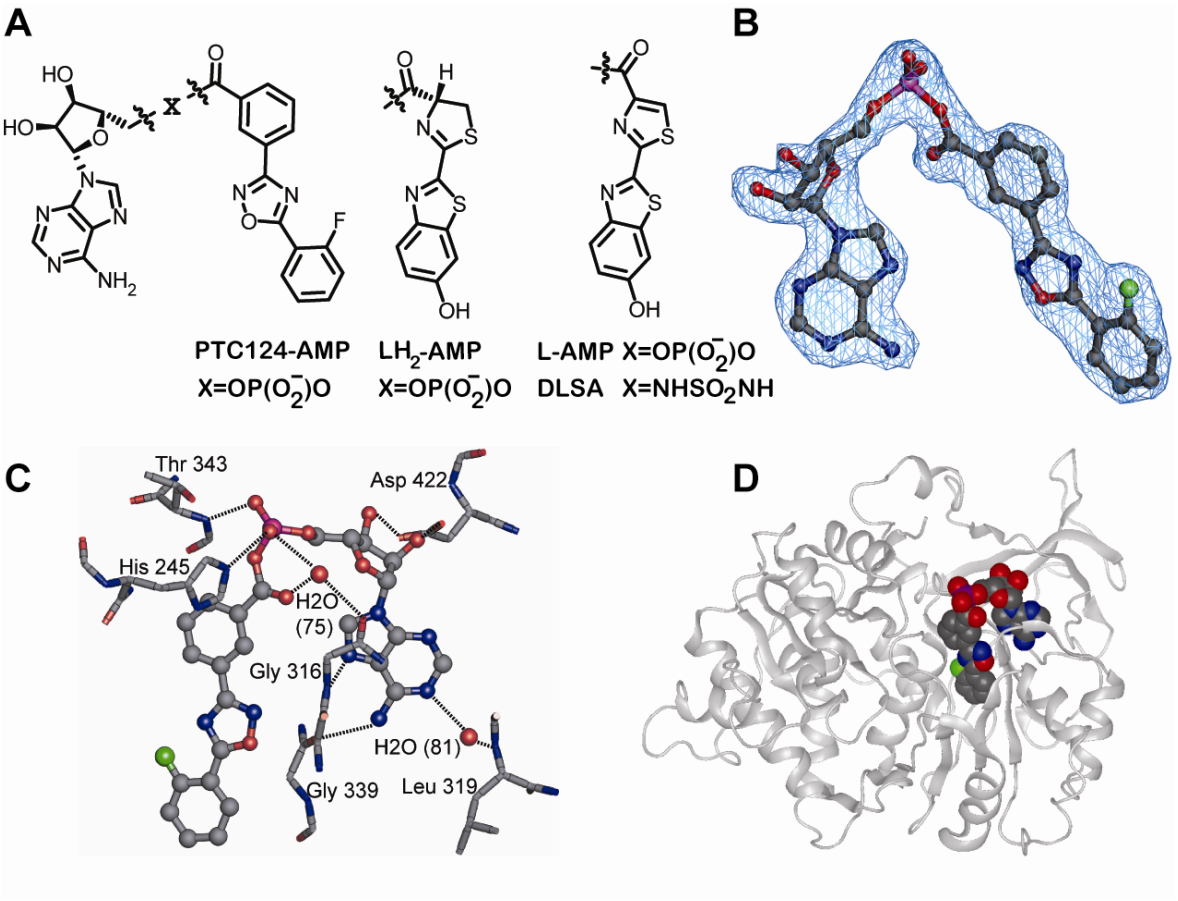

Douglas S. Auld, Scott Lovell, Natasha Thorne, Wendy A. Lea, David J. Maloney, Min Shen, Ganesha Rai, Kevin Battaile, Craig J. Thomas, Anton Simeonov, Robert P. Hanzlik, and James Inglese, "Molecular Basis for the High Affinity Binding and Stabilization of Firefly Luciferase by PTC124." Proc. Nat. Acad. Sci. USA 2010, 107, 4878-83. PMID 20194791. Publisher's official version: http://dx.doi.org/10.1073/pnas.0909141107

Figure 2

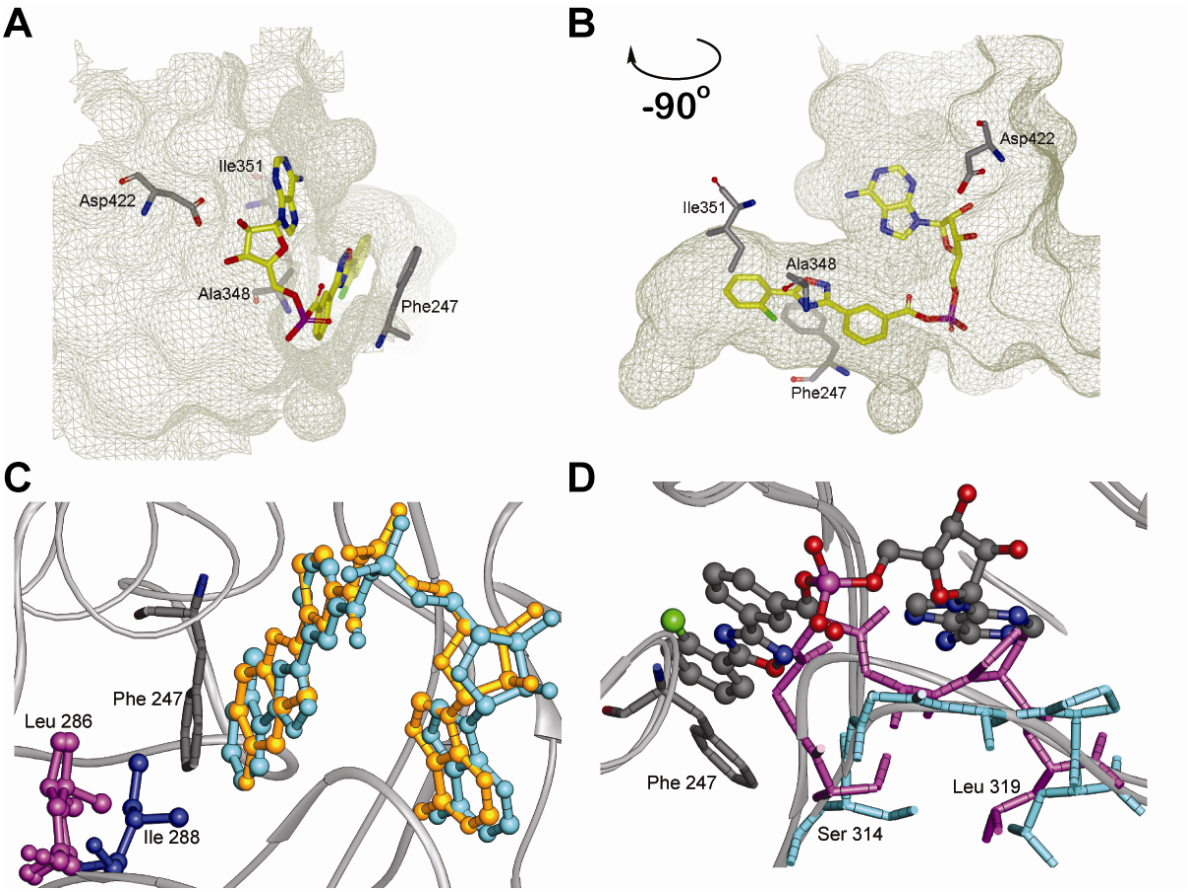

Douglas S. Auld, Scott Lovell, Natasha Thorne, Wendy A. Lea, David J. Maloney, Min Shen, Ganesha Rai, Kevin Battaile, Craig J. Thomas, Anton Simeonov, Robert P. Hanzlik, and James Inglese, "Molecular Basis for the High Affinity Binding and Stabilization of Firefly Luciferase by PTC124." Proc. Nat. Acad. Sci. USA 2010, 107, 4878-83. PMID 20194791. Publisher's official version: http://dx.doi.org/10.1073/pnas.0909141107

Figure 3

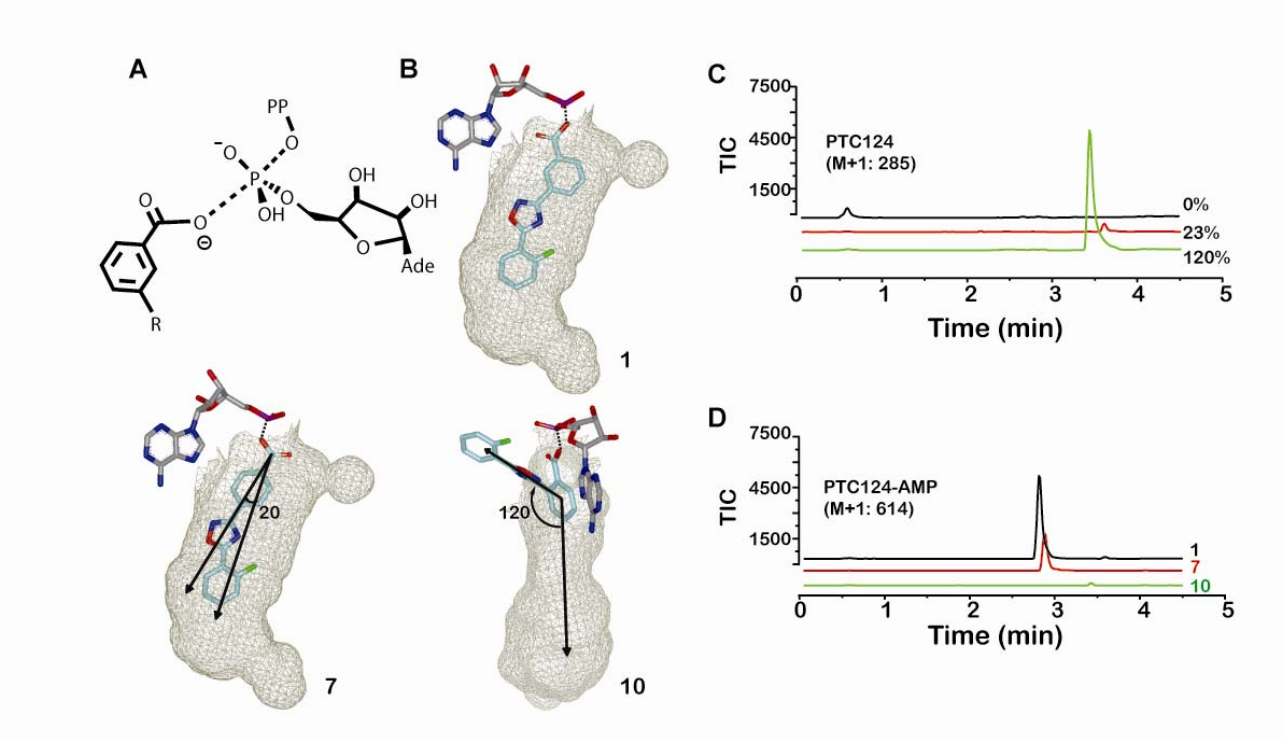

Douglas S. Auld, Scott Lovell, Natasha Thorne, Wendy A. Lea, David J. Maloney, Min Shen, Ganesha Rai, Kevin Battaile, Craig J. Thomas, Anton Simeonov, Robert P. Hanzlik, and James Inglese, "Molecular Basis for the High Affinity Binding and Stabilization of Firefly Luciferase by PTC124." Proc. Nat. Acad. Sci. USA 2010, 107, 4878-83. PMID 20194791. Publisher's official version: http://dx.doi.org/10.1073/pnas.0909141107

Figure 4

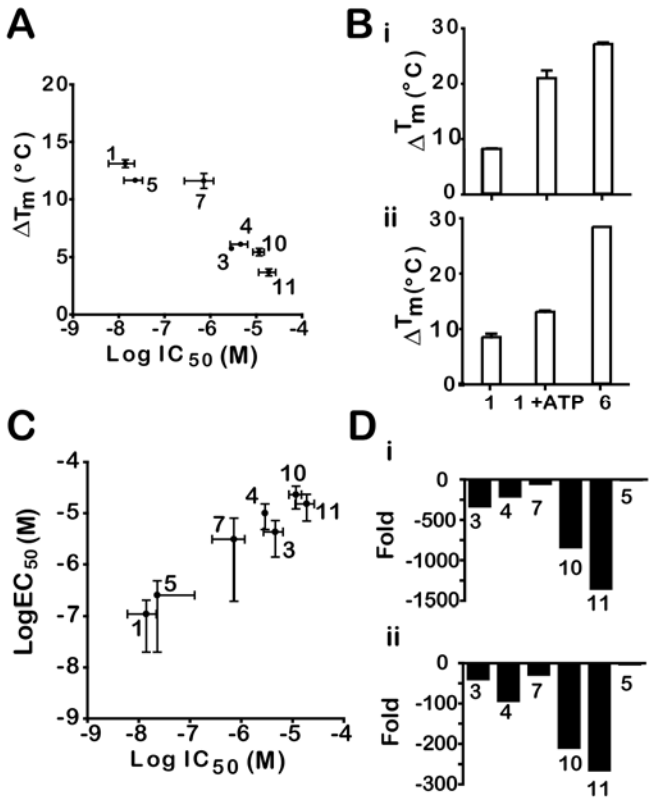

Douglas S. Auld, Scott Lovell, Natasha Thorne, Wendy A. Lea, David J. Maloney, Min Shen, Ganesha Rai, Kevin Battaile, Craig J. Thomas, Anton Simeonov, Robert P. Hanzlik, and James Inglese, "Molecular Basis for the High Affinity Binding and Stabilization of Firefly Luciferase by PTC124." Proc. Nat. Acad. Sci. USA 2010, 107, 4878-83. PMID 20194791. Publisher's official version: http://dx.doi.org/10.1073/pnas.0909141107

Table 1

R1	**R2**		**FLuc IC_{50} (μM)**	**$FLuc^{UGA}$ EC_{50} (μM)**	**$FLuc^{UGA}$ % Activation**
o-F	*m*-COOH	**(1)**	0.014 ± 0.008	0.11 ± 0.09	1345 ± 391%
o-F	H	**(2)**	0.99 ± 0.59	11.9 ± 5.8	812 ± 268%
o-F	*m*-$CONH_2$	**(3)**	4.6 ± 1.9*	4.3 ± 2.9	1019 ± 262%
o-F	*m*-tetrazole	**(4)**	2.9 ± 1.7	10.2 ± 5.2	618 ± 59%
m-Cl	*m*-COOH	**(5)**	0.023 ± 0.01	0.25 ± 0.23	1013 ± 319%
o-F	*m*-CO(AMP)	**(6)**	0.020 ± 0.01	N/A	N/A
o-F	*p*-COOH	**(7)**	0.72 ± 0.45	3.1 ± 4.9	1288 ± 510%
o-F	*p*-$CONH_2$	**(8)**	4.3 ± 2.0*	0.77 ± 0.05	1816 ± 982%
o-F	*p*-tetrazole	**(9)**	14.5 ± 5.0	16.5 ± 3.0	528 ± 189%
o-F	*o*-COOH	**(10)**	11.7 ± 3.2*	23.0 ± 10.8	369 ± 209%
o-F	*o*-$CONH_2$	**(11)**	18.9 ± 7.6*	8.2 ± 9.7	118 ± 92%
o-F	*m*-CONH(sa-Ade)	**(12)**	0.005 ± 0.001	N/A	N/A
o-F	*p*-CONH(sa-Ade)	**(13)**	0.003 ± 0.001	N/A	N/A

* = partial inhibition of FLuc observed, e.g. % inhibition (x) was 40% < x ≤ 80%
N/A = not applicable

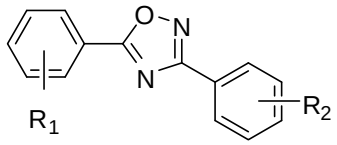

Douglas S. Auld, Scott Lovell, Natasha Thorne, Wendy A. Lea, David J. Maloney, Min Shen, Ganesha Rai, Kevin Battaile, Craig J. Thomas, Anton Simeonov, Robert P. Hanzlik, and James Inglese, "Molecular Basis for the High Affinity Binding and Stabilization of Firefly Luciferase by PTC124." Proc. Nat. Acad. Sci. USA 2010, 107, 4878-83. PMID 20194791. Publisher's official version: http://dx.doi.org/10.1073/pnas.0909141107

Supplemental Information

Molecular Basis for the High Affinity Binding and Stabilization of Firefly Luciferase by PTC124

Douglas S. Auld[a], Scott Lovell[b], Natasha Thorne[a], Wendy A. Lea[a], David J. Maloney[a], Min Shen[a], Ganesha Rai[a], Kevin Battaile[c], Craig J. Thomas[a], Anton Simeonov[a], Robert P. Hanzlik[b], and James Inglese[a, 1]

[a]NIH Chemical Genomics Center, National Institutes of Health, Bethesda, MD 20892-3370, USA

[b]Structural Biology Center, University of Kansas, 2121 Simons Drive, Lawrence, KS 66047

[c]IMCA-CAT, Advanced Photon Source, Argonne National Laboratory, 9700 South Cass Avenue, Bldg 435A, Argonne, IL 60439

[1]To whom correspondence should be addressed. E-mail: jinglese@mail.nih.gov, Phone: 301- 217-5722, Fax: 301-217-5736

Douglas S. Auld, Scott Lovell, Natasha Thorne, Wendy A. Lea, David J. Maloney, Min Shen, Ganesha Rai, Kevin Battaile, Craig J. Thomas, Anton Simeonov, Robert P. Hanzlik, and James Inglese, "Molecular Basis for the High Affinity Binding and Stabilization of Firefly Luciferase by PTC124." Proc. Nat. Acad. Sci. USA 2010, 107, 4878-83. PMID 20194791. Publisher's official version: http://dx.doi.org/10.1073/pnas.0909141107

Supplemental Figure Captions:

Figure S1. **Reactions catalyzed by FLuc**. **(A)**. FLuc catalyzes the reaction between D-luciferin and ATP to form the intermediate LH_2-AMP which eventually leads to production of oxyluciferin and light. A side-reaction involving oxidation of the LH_2-AMP intermediate forms L-AMP, which is an inhibitor of FLuc (specifically, a MAI). The "?" indicates that the exact mechanism of oxidation and the efficiency of this conversion is presently unknown. Potent inhibition of FLuc by L-AMP can be relieved through the thiolytic reaction of FLuc-bound L-AMP and Coenzyme A (CoASH), to form L-CoA, a significantly weaker inhibitor of FLuc (1). Figure adapted from Fraga et al., 2005 (1). **(B)** The FLuc enzyme catalyzed reaction of PTC124 and ATP to form the potent MAI PTC124-AMP. We predict that thiolysis can also occur between PTC124-AMP and CoASH, similar to that reported for L-AMP and CoASH, forming a PTC124-CoA product, which is significantly less inhibitory than PTC124-AMP.

Figure S2. MALDI-MS of FLuc. **(A)**. Luciferase purchased from Sigma. **(B)** Luciferase crystals obtained from Synergy #45 dissolved in 0.1% TFA/water. For the luciferase structure described here, we found that the residues in the C-terminal domain region near V435 to V551 in the full length model used for molecular replacement were not masked by electron density following refinement. In addition, the *B*-factors for the amino acids in this region refined to approximately 6-times that of the average value of the model indicating that these residues were disordered. The protein used for crystallization experiments, as well as the FLuc crystals themselves, displayed a peak near the expected 60 kDa MW of FLuc, indicating that the C-terminal residues were indeed disordered and not truncated. This is not unexpected as the C-terminal domain

appears to be dynamic when comparing previously determined structures of luciferase. For example, the structures from LcrLuc (2) and FLuc (3) are rather similar overall, while the C-terminal domains adopt dramatically different orientations relative to each other.

Figure S3. Comparison of FLuc structures and modeling of the PTC124-AMP adducts. (**A**) Overlay of PTC124-AMP (turquoise) and LcrLuc bound to DLSA (gold; PDB: 2D1S) showing the similarities of the ligand binding mode. Ile 288 from LcrLuc:DLSA is colored blue and Leu 286 from the FLuc structures (apo and bound) are colored magenta. Structures shown are rotated approximately 90° relative to **Fig. 2C** shown in main text. (**B**) Overlay of FLuc:PTC124-AMP (turquoise) with FLuc:Apo (magenta). The overall structures are quite similar with the exception of the loop region between Ser 314 and Leu 319 located between the asterisks. We also determined a second apo structure of FLuc (FLuc:Apo2; see PDB: 3IER), one that contains a polyethylene glycol 400 (PEG 400) molecule (a component of the crystallization solution) bound in the hydrophobic luciferin pocket. The binding of PEG 400 does not affect the conformation of the loop between Ser 314 and Leu 319, which is nearly identical to FLuc:Apo. For example, Ala 317 was disordered in FLuc:Apo2, and thus could not be modeled, and the *B*-factors for residues in this loop are nearly twice that of the average value of the model for apo structures unlike the PTC-AMP bound structure, where the B-factors for this loop are similar to the overall value for the model, with well defined electron density. (**C**) The *para*- and *ortho*-PTC124-AMP adducts (***i***, ***ii***, respectively) were modeled in the binding pocket defined by the co-crystal structure of

the PTC124-AMP adduct (gold structure). Molecular docking of the *para*- and *ortho*-PTC124-AMP adducts were performed using FRED. See ***SI* Methods** for details. This figure was prepared with the program VIDA (OpenEye Scientific Software). (**C, *iii***) illustrates how in the active site the carboxylate oxygen of PTC124 (*m*-isomer, shown in red) is ideally situated to form a NAC and displace pyrophosphate from ATP. However, when the diphenyloxadiazole moiety of the *p*-isomer (blue) is superimposed over that of the *m*-isomer (left side), the nucleophilic oxygen is too far away to form an efficient NAC. To locate the nucleophilic oxygen of the *p*-isomer requires a realignment of the long axis of the molecule by ca. 20˚ as shown on the right. Hence the *p*-isomer is much less effective than the *m*-isomer.

Figure S4. **LC-MS analysis of adenylate adduct formation by FLuc**. (**A**) Far left and middle graphs show the total ion current (TIC) data (PTC124 mass, top graphs; PTC124-AMP mass, bottom graphs) for incubation of 20 μM PTC124 in the presence of 2 mM ATP alone or with 20 μM FLuc and 2 mM ATP. The far right graph shows the TIC data for the synthetically made PTC-AMP in buffer alone. (**B**) The formation of PTC-AMP can be titrated by varying the enzyme concentration. The TIC for the PTC124 (left graph) and PTC-AMP (right graph) is shown at three different FLuc concentrations with 2 mM ATP present and 20 μM PTC124, incubation time ~10 min.

Figure S5. K_D determination for the PTC124-AMP:FLuc complex. A method to calculate the K_D defined as:

$$K_D = \frac{(E)_{free}(PTC124\text{-}AMP)_{free}}{E\text{-}PTC124\text{-}AMP}$$

used the derivation described by Rhodes *et al* (4) where we applied the linear equation shown below to obtain the K_D:

$$K_D = \frac{f}{1-f}(\text{PTC124-AMP})_{total} - f(E)_{total} \text{ where } f = \frac{E_{free}}{E_{total}}$$

The fraction (***f***) is directly calculated from the ratio of light intensities upon incubation of FLuc with LH2-AMP at varying concentrations of PTC124-AMP ligand. In the experiment, known concentrations of PTC124-AMP are added to a known concentration of FLuc (100 nM) and the light intensity is measured immediately after addition of LH2-AMP. From this linear plot E_{total} and K_D are obtained from the slope and intercept of the graph, respectively. From the plot shown we obtained an E_{total} = 43 nM and a K_D = 143 pM (average 130 ± 20 pM). r^2 for plot is 1.000. Ligand = PTC124-AMP.

Figure S6. Thermal Shift Profiles. We assessed the thermal profile of 1.8 μM FLuc in Tris-acetate buffer and obtained a T_m of 48.3°C ± 0.13 (a T_m of 48.5 °C ± 0.11 was obtained for FLuc in PBS)**.** Data shown is for a total of six replicates in all cases and the concentrations of the tested compound are noted in (**C**). **(A)** Thermal shift profile of 1.8 μM FLuc in the absence (**left)** and the presence **(right)** of 2 mM ATP. Shown are the individual profiles obtained from six replicates (n). (**B**) PTC124 thermal melting profiles in the absence (left graph) and presence (right graph) of 2 mM ATP at various concentrations of PTC124 ranging from 0.01 to 200 μM (alternate traces shown; see PubChem AID: XXX). A concentration-dependent increase in FLuc T_m was observed: marginal (<1.5 °C) T_m shift was detected below 1 μM compound, but the thermostability of the protein was augmented as the compound:protein ratio was increased, reaching a maximal stability (max ΔT_m) near the highest compound concentration tested (200 μM).

Thermal denaturation of 1.8 μM FLuc in the presence of increasing concentrations PTC-AMP in Tris buffer (**C**) or PBS buffer (**D**). For this compound, in the 5 μM-20 μM range, biphasic thermal melt curves were observed. At the next higher concentration, 20 μM, the two transitions coalesced yielding a single asymmetric peak which was skewed to the high temperature side. Such behavior has been previously reported for *Cypridina* luciferase using different detection methods as well as with other proteins, such as undefatted albumin with palmitate (5) and BSA with bis-ANS (6), and has been attributed to an increase in free ligand concentration due to the release of previously bound ligand by the protein during heat denaturation. The resulting redistribution of ligand occupies a lower-affinity site which is revealed at the higher temperatures (7, 8).

Figure S7. **Example of concentration-response curves**. (**A**) **Top**, nonsense codon suppression assay. Apparent activation of FLuc activity in the cell-based assay after 48-hour incubation of cells with PTC124 or analogs. The most potent compound is PTC124 (**1**) and the least potent compounds, which also demonstrate the weakest efficacies, are the *ortho*-substituted analogs (**10, 11**). This potency trend is mirrored in the purified enzyme assay (**bottom**). (**B-E**) Purified enzyme assay, CRCs in the presence or absence of 500 μM CoASH or 1 mM cysteine for PTC124 (**1; B**), and the *p*-carboxylate analog (**7; C**). CoASH appears to have the greatest effect on the potency of PTC124 (**1; B**), and little effect on the acylsulfamide *meta* and *para* adducts (**12** and **13**; **D**,**E**) consistent with a thiolytic mechanism.

Douglas S. Auld, Scott Lovell, Natasha Thorne, Wendy A. Lea, David J. Maloney, Min Shen, Ganesha Rai, Kevin Battaile, Craig J. Thomas, Anton Simeonov, Robert P. Hanzlik, and James Inglese, "Molecular Basis for the High Affinity Binding and Stabilization of Firefly Luciferase by PTC124." Proc. Nat. Acad. Sci. USA 2010, 107, 4878-83. PMID 20194791. Publisher's official version: http://dx.doi.org/10.1073/pnas.0909141107

Supplemental Methods.

Structure solution and refinement. The firefly luciferase protein (Sigma cat # L9506) was exchanged to the buffer previously described for crystallization of firefly luciferase (9) (200 mM $(NH_4)_2SO_4$, 1 mM EDTA, 1 mM DTT, 10% glycerol, 25% ethylene glycol, 25 mM Tris pH 7.8) and concentrated to 16.3 mg/mL. Crystallization trials were conducted in Compact Jr. sitting drop vapor diffusion plates (Emerald biosystems) using 0.5 µL of protein and 0.5 µL of crystallization screen solution equilibrated against 100µL reservoir solution. Crystals displaying a needle morphology were obtained with 24 hours at 4^{o}C from the Precipitant Synergy screen (Emerald biosystems) conditions #41 (25% PEG 400, 20% PEG 3350, 0.1 M $MgCl_2$, 0.1 M Tris pH 8.5) and #45 (30% PEG 1500, 8%(v/v) MPD, 0.1 M Tris pH 8.5). Crystals from Synergy #41 and #45 were soaked for 2 hours in fresh drops of crystallization solution containing 5 mM ATP and 5 mM PTC124 to prepare the adduct complex. Luc:Apo and Luc:Apo2 crystals were obtained from Synergy #45 and Synergy #41 respectively. All samples were frozen in their respective crystallization solutions which also served as a cryoprotectant.

All X-ray diffraction data were collected at the Advanced Photon Source (APS), IMCA-CAT beamline 17BM using an ADSC Quantum 210 CCD detector. Data were collected at 100K using an X-ray wavelength of 1.0000 Å. Data were integrated and scaled using HKL2000 (10). Structural comparison was performed using the least squares fitting procedure in Coot. Cα atoms were used for fitting. Figures were prepared using the Ribbons software package (11).

The unit cell parameters and space group for the luciferase crystals obtained in our laboratory were different from those reported for the two known *P. pyralis* structures

(PDB: 1LCI (3) and 1BA3 (12)) which both reportedly crystallized in the primitive tetragonal space group (13) $P4_12_12$. Based on the unit cell volume and molecular weight of 60,844.1 Da, the Matthew's coefficient (V_m) was calculated to be 2.83 $Å^3$/Da with equates to 56.5% solvent content for 1 molecule in the asymmetric unit. The initial structure of apo luciferase was solved by molecular replacement with MOLREP(13) in the space group $P4_1$ using 1LCI as the search model. Clear peaks were observed from the rotation and translation functions that were approximately 6 and 10 times greater than the background. This along with the observed correlation coefficient of 0.583 indicated that a clear solution had been found. Molecular replacement search in the enantiomorphous space group ($P4_3$) resulted in a correlation coefficient of 0.434 and resulted in high R factors (~50%) following refinement. Therefore, the solution obtained in the space group $P4_1$ was used for refinement. The initial model was refined with Refmac (14) which converged at R/R_{free} = 21% and 25% and the resulting electron density maps fit well with the overall model. Structures were manually built using Coot (15) and refined with Refmac. The final model was used for molecular replacement against subsequent data sets. Although the adduct complex could be prepared from crystals obtained from both crystallization solutions, those grown from Synergy #45, described above, diffracted to moderately higher resolution amongst the samples tested. Therefore, the data collected for the sample from Synergy #45 was used for final refinement and model building. For Luc:Apo2 (PDB: 3IER), residual difference electron density was observed in the hydrophobic pocket of the active site and was modeled as a PEG 400 molecule. The following Ramachandran plot statistics were

observed. Luc:Adduct (PDB: 3IES): core-91.4%, allowed-8.4%, Luc:Apo (PDB: 3IEP): core-91.5%, allowed-8.2%, Luc:Apo2: core-92.9%, allowed-6.8%.

LC-MS. Samples (10 µL injection) were analyzed on an Agilent 1200 series LC/MS equipped a Agilent 6130 Quadrupole MS detector and a Luna® C18 reverse phase (3 micron, 3 x 75mm) column having a flow rate of 1.0 mL/min. The mobile phase was a mixture of ACN (0.025% TFA) and H_2O (0.05% TFA), and column temperature was maintained at 50°C. A gradient of 4% to 100% ACN over 3 minutes was applied.

MALDI-TOF mass spectrometric analysis. Samples were submitted for analysis by MALDI-MS to determine if the luciferase crystals were composed of the expected 60,844.1 kDa protein. Additionally, the protein used for crystallization screening was tested for comparison. Analysis was performed using a MALDI-TOF mass spectrometer (PerSeptive Biosystems, Voyager-DE STR). The instrument was operated in a positive linear mode with following parameters: accelerating voltage 25 kV, grid voltage 95%, guide wire 0.05% and extraction delay time 50 nsec. Acquisition mass range was 5,000-90,000. Raw spectrum data were processed using Gaussian Smooth algorithm within the Data Explorer software (version 4.6). Crystals were transferred from their native drops and washed in three drops of crystallization solution to remove any soluble protein that might be transferred from the crystallization drop before dissolving in 0.1% TFA in water. Protein samples were desalted using reverse phase C4 ZipTips (Millipore, USA) and eluted with 50% acetonitrile / 0.1% TFA containing the matrix (sinapinic acid, saturated solution) onto a stainless steel MALDI sample plate. Analysis was performed using a MALDI-TOF mass spectrometer (PerSeptive Biosystems, Voyager-DE STR). The instrument was operated in a positive linear mode with

following parameters: accelerating voltage 25 kV, grid voltage 95%, guide wire 0.05% and extraction delay time 50 nsec. Acquisition mass range was 5,000-90,000. Raw spectrum data were processed using Gaussian Smooth algorithm within the Data Explorer software (version 4.6).

Molecular Modeling. FRED requires a set of input conformers for each ligand. The multiple low-energy conformers of the ligands were generated by OMEGA and stored in a single binary file. Partial charges were assigned to the ligands using MMFF94 force field (16). The default parameter values were used in OMEGA with two exceptions; the maximal number of low-energy conformations generated for each ligand was set to 1000, and the RMS threshold between different conformers was set to 0.5Å. The crystallographic structure of luciferase with PTC124-AMP bound was prepared for the docking studies using MOE molecular modeling software (17). All hydrogens were added to the protein and partial charges were attributed to the protein atoms using Amber99 force field (18). The docking boxes delineating the binding site were defined by the ligand PTC124-AMP from the luciferase crystal structures using FRED_receptor, a FRED docking preparation program. Each ligand conformation is rigidly optimized using shape and chemical complementarities of protein and ligand, followed by consensus scoring using a number of scoring functions. FRED rigidly docks the pregenerated conformations of each ligand into a nonflexible target protein to generate an optimal binding pose within the active site through the following consecutive steps: exhaustive docking, systematic solid body optimization of the top ranked candidate poses, ranking pose via consensus structure method, and optionally full coordinate

refinement of all ligand atoms using MMFF94 force field. In this work, the force field refinement was not used.

Thermal melting experiments. *P. pyralis* luciferase (FLuc) used in the thermal shift assay was procured from Sigma (catalog no. L1792). The fluorescent dye indicator SYPRO Orange, available at a stock concentration of 5000x, was obtained from Invitrogen, presently Life Technologies (Carlsbad, CA). This dye was used due to its low quantum yield in aqueous solution but high fluorescence in nonpolar environments. An increase in fluorescence indicates binding of the dye to hydrophobic regions of the protein which are exposed during protein unfolding. Accurate detection of fluorescent signal in these assays requires the use of high enzyme concentration. The final concentration of the enzyme and SYPRO Orange were maintained at 1.8 μM and 5x, respectively. The enzyme and the dye were separately made in either PBS (with or without 2 mM ATP) or Tris-acetate (with or without 2 mM ATP). Test compounds were originally dissolved as 10 mM stock solutions and were further diluted in DMSO, with the exception of the PTC124-AMP adduct which was prepared as 2.9 mM stock in phosphate-buffered saline (PBS, pH 7.4) and was further diluted in either PBS or 50 mM Tris-acetate buffer (pH 7.6). The dilution series were stored in mother plates, serving as source plates for the PCR plates used in DSF. For PTC124 and PTC124 analogs, 1 μL compound solution in DMSO (final concentrations ranging from 0.1 nM to 200 μM) was added to 49 μl FLuc-SYPRO Orange mixture in 96-well thin wall PCR plates (Bio-Rad, Hercules, CA). The final DMSO content was maintained at the suggested value of 2%. For the PTC124-AMP adduct, 9 μL compound solution (final concentrations: 1-500 μM), or 9 μL buffer as vehicle control, was added to 41 μL FLuc-

SYPRO Orange mixture. After sample mixing, the plates were centrifuged at 1,000 rpm for 10 seconds before being sealed with Optical-Quality Sealing Tape (Bio-Rad). The plates were then heated in an iQ5 Real Time PCR Detection system (Bio-Rad) from 20 to 95°C in increments of 1°C and a ramping rate of 0.1°C/s. The temperature ramp commenced approximately 2 min after sample mixing. Fluorescence intensity changes (Ex 490/Em 575 nm) were monitored with a charge-coupled device (CCD) camera (19).

Analysis of thermal shift data. The temperature midpoint of the protein unfolding transition, T_m, was obtained through a Boltzmann model using an Excel based worksheet provided by Niesen et al. (ftp://ftp.sgc.ox.ac.uk/pub/biophysics):

RFU = RFU1 + (RFU2-RFU1)/(1 + exp ((Tm – T)/slope)) equation (1), (19)

where RFU1 and RFU2 represent the minimum and maximum fluorescence intensities at temperatures at the two sides of the transition, respectively. The differences between the midpoints (T_m) of the thermal profiles of the control (samples with DMSO or carrier buffer without compounds) and compound-containing samples were calculated to yield thermal shifts (ΔT_m).

Cell-based FLuc nonsense codon suppression assays: Grip-Tite cells transiently transfected according to standard procedure (TransFast Transfection Reagent; Promega; cat# E2431) with the pFLuc190^{UGA} construct were seeded in white solid-bottom tissue culture-treated 1,536-well microplates (Greiner Bio-One) at a density of 6.7 x 10^5 cells/mL in a volume of 6µL per well (~4000 cells/well) using the BioRAPTR Flying Reagent Dispenser (FRD; Aurora Discovery). Plates were then incubated for one hour at 37ºC, 95% humidity, 5% CO_2. These assay plates were then treated with 23nL

of compound or DMSO using a Kalypsys pin tool with a 1,536-array of 10nL slotted pins. This allowed the delivery of a 24-point titration of each compound to the assay plate, with a final compound concentration ranging from approximately 40μM to 5pM. Assay plates were then incubated for 48 hours. Following incubation, GripTite cells were washed with DPBS (3X; 7uL/wash; Invitrogen; 14040) using a Multidrop Combi (Thermo Fisher Scientific) followed by removal of liquid by brief centrifugation. A final volume of 6μL of DPBS was delivered to each well before addition of 3uL of 3X detection reagent (contains 100mM Tris-HCl, 40mM Tris-Base, 3mM MgCl, 3% Triton-X, 15mM DTT, 1.5mM CoA, 450uM ATP, and 1.4mM D-luciferin and prepared in house) using the FRD. Luciferase activity was then measured using a ViewLux CCD imager (PerkinElmer), with an exposure time of 120s.

General Synthetic Methods: Unless otherwise stated, all reactions were carried out under an atmosphere of dry argon or nitrogen in dried glassware. Indicated reaction temperatures refer to those of the reaction bath, while room temperature (rt) is noted as 25 ^{o}C. All solvents were of anhydrous quality purchased from Aldrich Chemical Co. and used as received. Commercially available starting materials and reagents were purchased from Aldrich, TCI and Acros and were used as received. If needed, products were purified via a Waters semi-preparative HPLC equipped with a Phenomenex Luna® C18 reverse phase (5 micron, 30 x 75 mm) column having a flow rate of 45 mL/min. The mobile phase was a mixture of acetonitrile and H_2O each containing 0.1% trifluoroacetic acid. Samples were analyzed for purity on an Agilent 1200 series LC/MS equipped with a Luna® C18 reverse phase (3 micron, 3 x 75 mm) column having a flow rate of 0.8-1.0 mL/min. The mobile phase was a mixture of acetonitrile (0.025% TFA)

and H_2O (0.05% TFA), and a temperature was maintained at 50 ^oC. A gradient of 4% to 100% acetonitrile over 7 minutes was used for purity analysis. Purity of final compounds was determined to be >95%, using a 3 µL injection with quantitation by AUC at 220 and 254 nM.

Analytical thin layer chromatography (TLC) was performed with Sigma Aldrich TLC plates Aldrich TLC plates (5 x 20 cm, 60 Å, 250 µm). Visualization was accomplished by irradiation under a 254 nm UV lamp. Chromatography on silica gel was performed using forced flow (liquid) of the indicated solvent system on Biotage KP-Sil pre-packed cartridges and using the Biotage SP-1 automated chromatography system. ^1H- and ^{13}C NMR spectra were recorded on a Varian Inova 400 MHz spectrometer. Chemical shifts are reported in ppm with the solvent resonance as the internal standard ($CDCl_3$ 7.26 ppm, 77.00 ppm, DMSO-d_6 2.5 ppm, 39.51 ppm for ^1H, ^{13}C respectively). Data are reported as follows: chemical shift, number of protons, multiplicity (s = singlet, d = doublet, dd = doublet of doublet, t = triplet, q = quartet, br = broad, m = multiplet), coupling constants. Low resolution mass spectra (electrospray ionization) were acquired on an Agilent Technologies 6130 quadrupole spectrometer coupled to an Agilent Technologies 1200 series HPLC. High resolution mass spectral data was collected in-house using and Agilent 6210 time-of-flight mass spectrometer, also coupled to an Agilent Technologies 1200 series HPLC system.

Douglas S. Auld, Scott Lovell, Natasha Thorne, Wendy A. Lea, David J. Maloney, Min Shen, Ganesha Rai, Kevin Battaile, Craig J. Thomas, Anton Simeonov, Robert P. Hanzlik, and James Inglese, "Molecular Basis for the High Affinity Binding and Stabilization of Firefly Luciferase by PTC124." Proc. Nat. Acad. Sci. USA 2010, 107, 4878-83. PMID 20194791. Publisher's official version: http://dx.doi.org/10.1073/pnas.0909141107

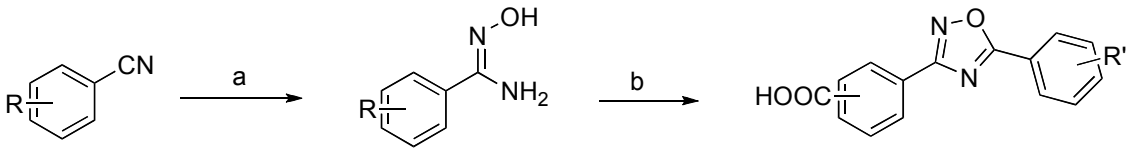

R=3'-$COOCH_3$
or 4'-$COOCH_2CH_3$

R'= - F, -Cl, -OCH_3, or -CF_3

Reagents and conditions: (a) NH_2OH, HCl, Hunig's Base, CH_2Cl_2, 40°C, 85-90%; (b) (i) R'-C_6H_4COCl, DIEA, DME, rt; (ii) DME, 100°C; (iii) LiOH, 2:1 THF/H_2O, rt, 50-90%.

Synthesis of PTC124 and analogues. The solution-phase synthesis of PTC124 (**1**) was accomplished utilizing methods similar to reported protocols (20, 21). The final three transformations (coupling of (*N*'-hydroxycarbamimidoyl)benzoates with substituted benzoyl chloride, cyclization to form oxadiazole, and ester deprotection) were accomplished using a modified one-pot method.

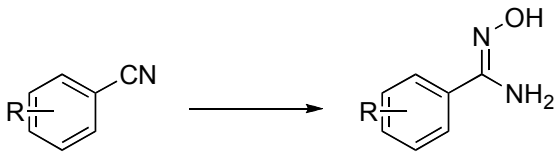

(*Z*)-alkyl-[3-or-4]-(*N*'-hydroxycarbamimidoyl)benzoates. To a solution of either methyl 3-cyanobenzoate or ethyl 4-cyanobenzoate (1 equivalent) in ethanol (2mL/mmol cyanobenzoate) was added hydroxylamine hydrochloride (1.5 equivalents) and diisopropylethylamine (2 equivalents). The mixture was heated to 40° C and allowed to stir for 18 hours, monitored by TLC for the disappearance of starting material. An excess of icewater was then added, and the resulting precipitate was collected via filtration, washed with water and ether, and allowed to dry. No further purification was needed and yields ranged from 85-90%.

Douglas S. Auld, Scott Lovell, Natasha Thorne, Wendy A. Lea, David J. Maloney, Min Shen, Ganesha Rai, Kevin Battaile, Craig J. Thomas, Anton Simeonov, Robert P. Hanzlik, and James Inglese, "Molecular Basis for the High Affinity Binding and Stabilization of Firefly Luciferase by PTC124." Proc. Nat. Acad. Sci. USA 2010, 107, 4878-83. PMID 20194791. Publisher's official version: http://dx.doi.org/10.1073/pnas.0909141107

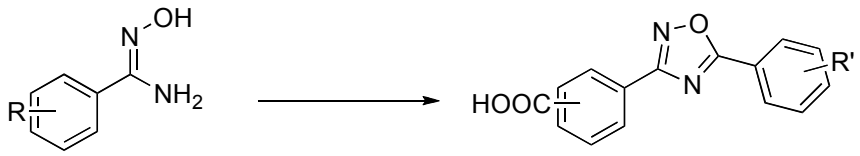

5-Phenyl substituted [3-or-4]-(5-phenyl-1,2,4-oxadiazol-3-yl)benzoic acids:

To a solution of either (*Z*)-methyl-3-(*N*'-hydroxycarbamimidoyl)benzoate or (*Z*)-ethyl-4-(*N*'-hydroxycarbamimidoyl)benzoate (1 equivalent) in 1,2-dimethoxyethane (3 mL/mmol) was added diisopropylethylamine (1.5 equivalents) and the solution was cooled to 5 ºC. To this mixture was added one of numerous substituted benzoyl chlorides (typical substitutions were F, Cl, and CF_3 at the ortho, meta and para positions, 1.2 equivalents) dropwise over a 20 min period. The mixture was allowed to warm to room temperature and was stirred for 4 h. The resulting mixture was heated at 100 ˚C for 12 h in a sealed reaction vessel. The reaction was then cooled to room temperature, and the solvent was removed under reduced pressure. The crude mixture was taken up in 2:1 THF/water (3 mL/mmol), and lithium hydroxide monohydrate (6 equivalents) was added. The reaction mixture was stirred for 3 h at room temperature, after which the organic solvent was removed under reduced pressure. The residue was dissolved in ethyl acetate and washed with 10% aq. HCl. The organic layer was separated, dried ($MgSO_4$), filtered and concentrated to afford generally pure products. If needed, products were further purified via a Waters semi-preparative HPLC equipped with a Phenomenex Luna® C18 reverse phase (5 micron, 30 x 75 mm) column having a flow rate of 45 mL/min. The mobile phase was a mixture of acetonitrile and H_2O each containing 0.1% trifluoroacetic acid. Pure fractions were concentrated and dried using

Glas-Col N_2 blowdown unit at 40 °C. Typical overall product yields ranged from 40-90%.

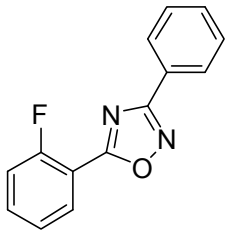

(2). 5-(2-fluorophenyl)-3-phenyl-1,2,4-oxadiazole

See procedure described above:

LC-MS: rt (min) = 6.73; ^{1}H NMR (400 MHz-DMSO-d_6) δ 7.42-7.61 (m, 5H), 7.72-7.78 (m, 1H), 8.05 (m, 2H) and 8.17 (m, 1H); ^{13}C NMR (400 MHz-DMSO-d_6) δ 111.67, 111.79, 117.10, 117.30, 125.33, 125.37, 125.92, 127.06, 129.17, 130.76, 131.60, 135.50 and 135.59; (Additional peaks are due to splitting with *o*-Fluoro group); HRMS (*m/z*): $[M]^+$ calcd. for $C_{14}H_9FN_2O$, 240.0699; found, 240.0696.

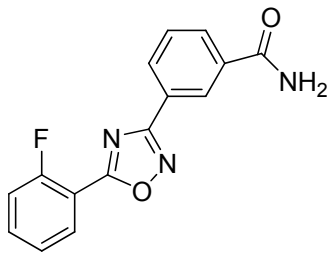

(3). 3-(5-(2-fluorophenyl)-1,2,4-oxadiazol-3-yl)benzamide:

To a solution containing 3-(5-(2-fluorophenyl)1-,2,4-oxadiazol-3-yl)benzoic acid (0.150 g, 0.53 mmol) in anhydrous CH_2Cl_2 (4 mL) at 0 ^oC was added oxalyl chloride (0.092 mL, 1.05 mmol) followed by cat. DMF. The reaction mixture was warmed to room temperature and stirred for 1.5 h. After this time the reaction mixture was concentrated under reduced pressure and dried under high vacuum. The residue was re-dissolved in dioxane (4 mL) and 30% NH_3 in water (10 equiv) was added dropwise. After 10 minutes the reaction mixture was diluted with ethyl acetate and washed with brine. The organic layer was separated, dried ($MgSO_4$) filtered and concentrated under diminished pressure. No further purification was required. yield: 0.148 g, 99%.; LC-MS: rt (min) = 5.12; ^1H NMR (400 MHz-DMSO-d_6) δ 7.50 (td, 1H, J = 7.6 and 1.2 Hz), 7.55 (m, 2H), 7.71 (td, 1H, J = 8.0 and 0.4 Hz), 7.81 (m, 1H), 8.11 (m, 1H), 8.24 (m, 3H) and 8.60 (m, 1H); ^{13}C NMR (400 MHz-DMSO-d_6) δ 111.67, 111.78, 117.32, 125.43, 125.58, 126.09, 126.34, 126.43, 129.31, 129.42, 129.68, 130.44, 130.91, 135.30, 135.78, 158.68, 161.24, 166.98, 167.68, 172.62 and 172.66; (Additional peaks are due to splitting with *o*-Fluoro group) HRMS (*m/z*): $[M]^+$ calcd. for $C_{15}H_{10}FN_3O_2$, 283.0757; found, 283.0759.

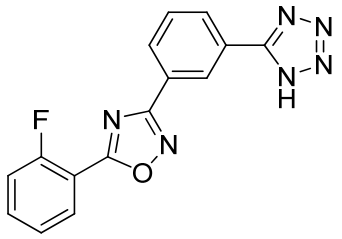

(4). 3-(3-(1H-tetrazol-5-yl)phenyl)-5-(2-fluorophenyl)-1,2,4-oxadiazole:

To a solution containing 0.050 g (0.19 mmol) of 3-(5-(2-fluorophenyl)-1,2,4-oxadiazol-3-yl) benzonitrile in DMF (1.5 mL) was added 0.074 g (1.13 mmol) of sodium azide followed by 0.10 g (1.89 mmol) of ammonium chloride. The reaction mixture was

heated to 90 ^{o}C for 24 h under a nitrogen atmosphere. After this time the reaction was cooled to room temperature, diluted with 0.5 mL of DMSO and filtered through a syringe filter. The filtrate was purified via a Waters semi-preparative HPLC equipped with a Phenomenex Luna® C18 reverse phase (5 micron, 30 x 75 mm) column having a flow rate of 45 mL/min. The mobile phase was a mixture of acetonitrile and H_2O each containing 0.1% trifluoroacetic acid. The product was collected as a colorless solid after lyophilization: yield 0.052 mg (89%); LC-MS: rt (min) = 5.62; ^{1}H NMR (400 MHz-DMSO-d_6) δ 7.52 (td, 1H, *J* = 6.8 and 1.2 Hz), 7.57 (ddd, 1H, *J* = 10.8, 8.4 and 0.8 Hz), 7.81 (m, 1H), 7.85 (t, 1H, *J* = 7.6 Hz), 8.28 (m, 3H) and 8.78 (t, 1H, *J* = 1.6 Hz); ^{13}C NMR (400 MHz-DMSO-d_6) δ 111.63, 111.74, 117.23, 117.44, 125.37. 125.51, 125.54, 127.11, 129.52, 129.95, 130.62, 130.92, 135.80, 135.89, 158.69, 161.25, 167.38, 172.77 and 172.81; (Additional peaks are due to splitting with *o*-Fluoro group) HRMS (*m/z*): $[M]^{+}$ calcd. for $C_{15}H_9FN_6O$, 308.0822; found, 308.0823.

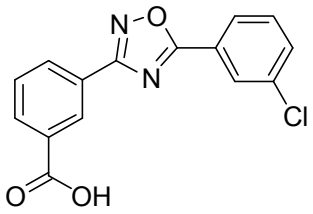

(**5**). **3-(5-(3-chlorophenyl)-1,2,4-oxadiazol-3-yl)benzoic acid:**

See procedure described above:

LC-MS: rt (min) = 6.73; ^{1}H NMR (400 MHz-DMSO-d_6) δ 7.68 (t, 1H, *J* = 8.0 Hz), 7.72 (t, 1H, *J* = 8.0 Hz), 7.79 (ddd, 1H, *J* = 8.0, 2.0 and 0.8 Hz), 8.14-8.18 (m, 3H), 8.30 (dt, 1H,

J = 8.0 and 1.6 Hz), 8.61 (t, 1H, *J* = 1.6 Hz) and 13.33 (brs, 1H); ^{13}C NMR (400 MHz-DMSO-d_6) δ 125.08, 126.29, 126.67, 127.40, 127.73, 129.81, 131.07, 131.55, 131.78, 132.27, 133.20, 134.16, 166.45, 167.72 and 174.42; HRMS (*m/z*): $[M]^+$ calcd. for $C_{15}H_9ClN_2O_3$, 300.0302; found, 300.0306.

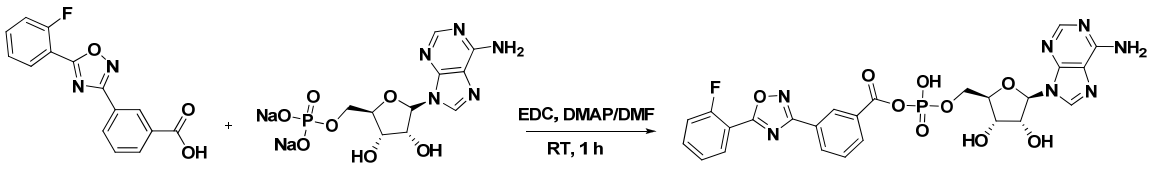

(6). PTC 124-AMP adduct:

A mixture of 3-(5-(2-fluorophenyl)-1,2,4-oxadiazol-3-yl)benzoic acid 0.2 g (0.70 mmol) and EDC 0.67 g (3.52 mmol) in anhydrous DMF (4 mL) was stirred at room temperature for 10 minutes. Then adenosine-5-monophosphate disodium salt 0.275 g (0.70 mmol) and DMAP 9 mg (0.07 mmol) were added and stirred vigorously at room temperature for 1 h. The crude product was purified in preparative HPLC and lyophilized to get the free acid as a white powder. The free acid was then dissolved in 0.1 molar ammonium bicarbonate solution and lyophilized to get the ammonium salt of the PTC-AMP adduct. LC-MS: rt (min) = 4.19; ^{1}H NMR (400 MHz-D_2O) δ 4.33-4.52 (m, 4H), 4.66 (t, 1H, *J* = 5.6 Hz), 5.88 (d, 1H, *J* = 5.6 Hz), 7.18-7.28 (m, 2H), 7.39 (t, 1H, *J* = 7.8 Hz), 7.60 (q, 1H, *J* = 13.6 Hz and 6.8 Hz), 7.71 (s, 1H), 7.80 (t, 1H, *J* = 7.2 Hz), 7.86-7.91 (m, 2H), 7.95 (s, 1H), 8.13 (s, 1H); ^{13}C-NMR (400 MHz-D_2O) δ 41.5, 66.4, 70.0, 73.9, 83.3, 83.4, 86.5, 110.6, 110.7, 116.8, 117.0, 117.7, 125.0, 125.2, 128.1, 129.2, 129.3, 129.4, 130.2, 131.7, 132.7, 135.7, 135.8, 148.3, 152.1, 154.6, 158.8, 161.3, 162.8, 162.9, 166.7, 172.67 and 172.72 (Additional peaks are due to splitting with *o*-Fluoro group); HRMS (*m/z*): $[M]^+$ calcd. for $C_{25}H_{21}FN_7O_9P$, 613.1122; found, 613.1128.

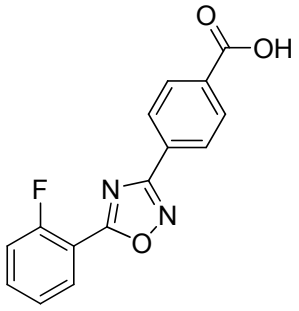

(7). 4-(5-(2-fluorophenyl)-1,2,4-oxadiazol-3-yl)benzoic acid:

See procedure described above:

LC-MS: rt (min) = 5.78; ^{1}H NMR (400 MHz-DMSO-d_6) δ 7.49 (td, 1H, J = 7.6 and 0.8 Hz), 7.54 (ddd, 1H, J = 10.8, 8.4 and 0.8 Hz), 7.80 (m, 1H), 8.12 (m, 2H), 8.22 (m, 3H) and 13.27 (brs, 1H); ^{13}C NMR (400 MHz-DMSO-d_6) δ 111.65, 111.76, 117.21, 117.42, 125.49, 125.52, 127.03, 128.28, 128.39, 130.89, 135.73, 135.82, 137.06, 158.68, 161.25, 167.04, 167.51, 172.64 and 172.69; (Additional peaks are due to splitting with *o*-Fluoro group) HRMS (*m/z*): $[M]^+$ calcd. for $C_{15}H_9FN_2O_3$, 284.0597; found, 284.0601.

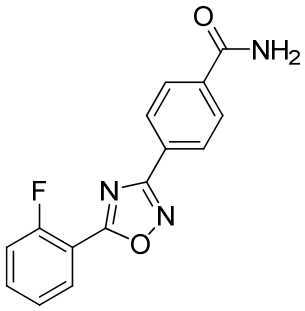

(8). 4-(5-(2-fluorophenyl)-1,2,4-oxadiazol-3-yl)benzamide:

See procedure described above:

LC-MS: rt (min) = 5.16; ^{1}H NMR (400 MHz-DMSO-d_6) δ δ 7.49 (td, 1H, J = 7.6 and 0.8 Hz), 7.53 (brs, 1H), 7.55 (ddd, 1H, J = 11.2, 8.4 and 0.8 Hz), 7.80 (m, 1H), 8.06 (m,

2H), 8.15 (m, 3H) and 8.23 (td, 1H, *J* = 7.6 and 1.6 Hz); ^{13}C NMR (400 MHz-DMSO-d_6) δ 111.65, 111.76, 117.21, 117.42, 125.49, 125.52, 127.03, 128.28, 128.39, 130.89, 135.73, 135.82, 137.06, 158.68, 161.25, 167.04, 167.51, 172.64 and 172.69; (Additional peaks are due to splitting with *o*-Fluoro group) HRMS (*m/z*): $[M]^+$ calcd. for $C_{15}H_{10}FN_3O_2$, 283.0757; found, 283.0755.

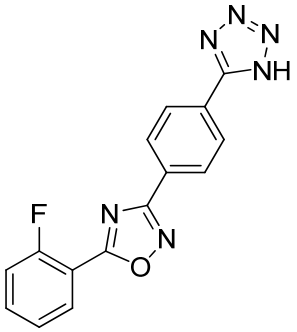

(9). 3-(4-(1H-tetrazol-5-yl)phenyl)-5-(2-fluorophenyl)-1,2,4-oxadiazole:

See procedure described above:

LC-MS: rt (min) = 5.63; ^{1}H NMR (DMSO-d_6) δ 7.50 (m, 1H), 7.54 (ddd, 1H, *J* = 11.2, 8.4 and 1.2 Hz), 7.80 (m, 1H) and 8.20-8.30 (m, 5H); ^{13}C NMR (DMSO-d_6) δ 111.62, 111.73, 117.15, 117.36, 125.46, 125.58, 127.36, 127.77, 128.10, 130.87, 135.72, 155.42, 158.69, 161.26, 167.37, 172.70 and 172.74; (Additional peaks are due to splitting with *o*-Fluoro group) HRMS (*m/z*): $[M]^+$ calcd. for $C_{15}H_9FN_6O$, 308.0822; found, 308.0821.

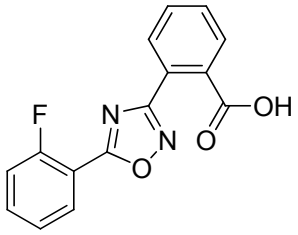

(10). 2-(5-(2-fluorophenyl)-1,2,4-oxadiazol-3-yl)benzoic acid:

See procedure described above:

LC-MS: rt (min) = 5.11; ^{1}H NMR (400 MHz-DMSO-d_6) δ 7.48 (td, 1H, *J* = 8.0 and 1.2 Hz), 7.53 (ddd, 1H, *J* =10.8, 8.4 and 0.8 Hz), 7.69-7.81 (m, 4H), 7.81-7.91 (m, 1H) and 8.17 (td, 1H, *J* = 7.6 and 2.0 Hz); ^{13}C NMR (400 MHz-DMSO-d_6) δ 111.58, 111.70, 117.24, 117.44, 125.52, 125.56, 125.87, 129.53, 130.23, 130.78, 131.11, 131.49, 133.00, 135.67, 135.76, 158.61, 161.18, 167.91, 168.68, 171.55 and 171.59; (Additional peaks are due to splitting with *o*-Fluoro group) HRMS (*m/z*): $[M]^+$ calcd. for $C_{15}H_9FN_2O_3$, 284.0597; found, 308.0593.

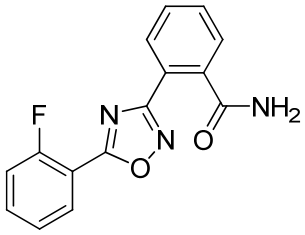

(11). 2-(5-(2-fluorophenyl)-1,2,4-oxadiazol-3-yl)benzamide:

See procedure described above:

LC-MS: rt (min) = 4.67; ^{1}H NMR (400 MHz-DMSO-d_6) δ 7.47 (brs, 1H), 7.49 (td, 1H, *J*, 8.0 and 1.2 Hz), 7.54 (ddd, 1H, *J* = 10.8, 8.4, and 0.8 Hz), 7.63 (m, 3H), 7.80 (m, 2H), 7.94 (brs, 1H) and 8.17 (td, 1H, *J* = 7.6 and 1.6 Hz); ^{13}C NMR (400 MHz-DMSO-d_6) δ

111.67, 111.79, 117.22, 117.43, 124.32, 125.49, 125.53, 128.05, 129.72, 129.78, 130.74, 130.80, 135.58, 135.67, 137.87, 158.58, 161.14, 168.43, 169.47, 171.49 and 171.54; (Additional peaks are due to splitting with *o*-Fluoro group) HRMS (*m/z*): $[M]^+$ calcd. for $C_{15}H_{10}FN_3O_2$, 283.0757; found, 283.0756.

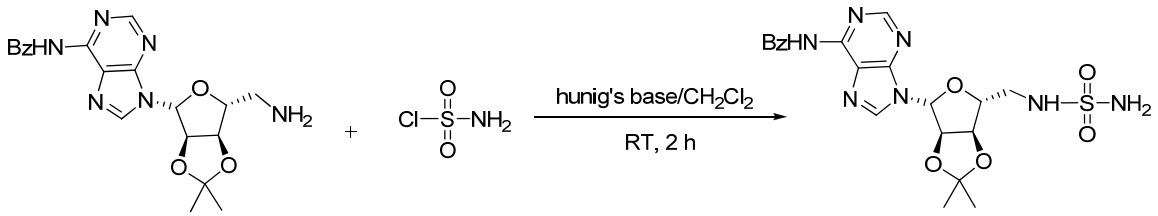

N-(9-((3aR,4S,6R,6aR)-2,2-dimethyl-6-((sulfamoylamino)methyl)tetrahydrofuro[3,4-d][1,3]dioxol-4-yl)-9H-purin-6-yl)benzamide: To a solution containing N-(9-((3aR,4R,6R,6aR)-6-(aminomethyl)-2,2-dimethyltetrahydrofuro[3,4-d][1,3]dioxol-4-yl)-9H-purin-6-yl)benzamide (22-24) (1 g, 1 eq, 2.44 mmol) and Hunig's base (0.85 mL, 2 eq, 4.88 mmol) in dichoromethane (15 mL) was added sulfamoyl chloride (23) (0.422 g, 1.5 eq, 0.85 mL) at 0 ^{o}C. The reaction mixture was allowed to stir at room temperature for 3 h. The solvent was evaporated and the crude product was purified on a Biotage® silica gel column using 5 % methanol in dichloromethane, providing the product as a colorless solid: Yield 0.6 g (2.44 mmol, 47 %). The product was used immediately in the next reaction.

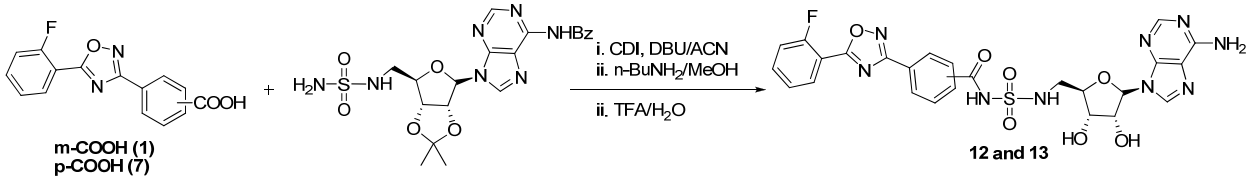

Synthesis of 12 and **13:** A 3/4-(5-(2-fluorophenyl)-1,2,4-oxadiazol-3-yl)benzoic acid (**1** or **7** respectively) (0.969 g, 3.41 mmol, 3 eq) and CDI (0.663 g, 4.09 mmol, 3.6 eq) in acetonitrile (15 mL) was dissolved by heating for 1 h at 60 ^{o}C. After cooling, a solution of (0.556 g, 1.136 mmol, 1eq) and DBU (0.26 mL, 1.7 mmol, 1.5 eq) in acetonitrile (15 mL) was added. The reaction mixture was stirred at 60 ^{o}C for 1 h. The solvent was evaporated and the crude product was purified on a preparative HPLC. The dry white

product was then stirred at room temperature for 1 h in a mixture of *n*-butylamine (5 mL) and methanol (5 mL). The solvent was evaporated and the crude product was stirred in a mixture TFA (7 mL) and water (4 mL) at RT for 1 h. The solvent was evaporated and the crude product was finally purified on a preparative HPLC and lyophilized providing the product as a colorless solid.

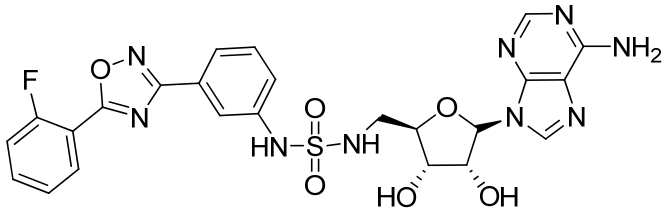

_N_-(_N_-(((2_R_,3_S_,4_R_,5_S_)-5-(6-amino-9H-purin-9-yl)-3,4-dihydroxytetrahydrofuran-2-yl)methyl)sulfamoyl)-3-(5-(2-fluorophenyl)-1,2,4-oxadiazol-3-yl)benzamide (12)

LC-MS: rt (min) = 4.37; ^{1}H NMR (DMSO-d_6) δ 4.12-4.16 (m, 2H), 4.17 (m, 6H), 4.66 (m, 1H), 5.86 (d, 1H, J = 6.4 Hz), 7.48-7.59 (m, 2H), 7.72 (t, 1H, J = 7.6 Hz), 7.78-7.84 (m, 1H), 8.11-8.13 (m, 1H), 8.24-8.32 (m, 2H), 8.37 (s, 1H), 8.48 (s, 1H), 8.57 (t, 1H, J = 1.6 Hz), 8.92 (brs, 1H) and 12.20 (brs, 1H); ^{13}C-NMR (DMSO-d_6) δ 45.1, 71.2, 72.8, 83.7, 88.4, 111.6, 111.7, 119.4, 125.5, 125.6, 126.3, 126.9, 129.7, 130.0, 131.1, 131.2, 132.0, 135.8, 135.9, 148.2, 149.0, 153.4, 158.2, 158.5, 158.7, 161.3, 164.8, 167.4, 172.75 and 172.79 (Additional peaks are due to splitting with *o*-Fluoro group); HRMS (ESI) *m*/*z* 612.1419 $(M+H)^+$ ($C_{25}H_{23}FN_9O_7S$ requires 612.1420).

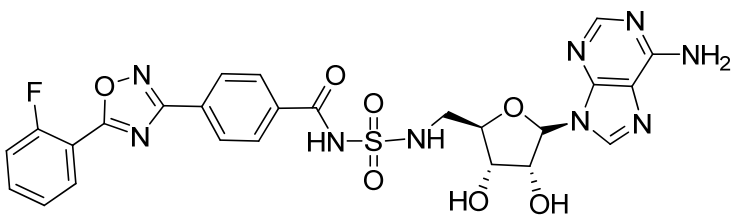

_N_-(_N_-(((2_R_,3_S_,4_R_,5_S_)-5-(6-amino-9H-purin-9-yl)-3,4-dihydroxytetrahydrofuran-2-yl)methyl)sulfamoyl)-4-(5-(2-fluorophenyl)-1,2,4-oxadiazol-3-yl)benzamide (13)

LC-MS: rt (min) = 4.11; ^{1}H NMR (DMSO-d_6) δ 3.62-4.26 (m, 2H), 4.66-4.69 (m, 5H), 7.49-7.59 (m, 2H), 7.79-7.84 (m, 1H, J = 7.6 Hz,), 8.09 (d, 2H, J = 8.4 Hz,), 8.18 (d, 2H, J = 8.0 Hz,), 8.23-8.28 (m, 1H), 8.35 (s, 1H), 8.45 (s, 1H), 8.99 (brs, 1H) and 12.09 (brs, 1H); ^{13}C-NMR (DMSO-d_6) δ 45.16, 71.24, 72.10, 83.64, 88.45, 111.63, 111.74, 114.67, 117.24, 117.45, 119.40, 125.53, 125.60, 127.15, 129.16, 129.58, 130.93, 134.6, 135.83, 135.92, 141.54, 148.29, 149.67, 153.93, 158.71, 161.28, 164.86, 167.30, 172.79 and 172.84 (Additional peaks are due to splitting with _o_-Fluoro group); HRMS (ESI) _m/z_ 612.1423 $(M+H)^+$ ($C_{25}H_{23}FN_9O_7S$ requires 612.1420).

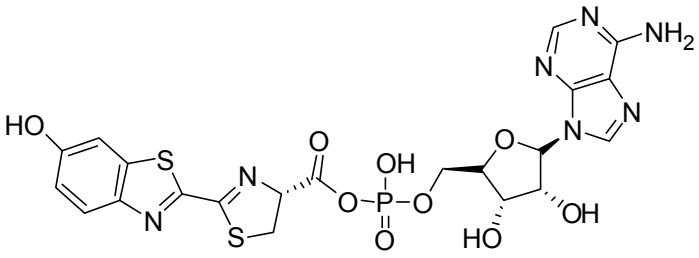

(((2S,3S,4R,5S)-5-(6-amino-9H-purin-9-yl)-3,4-dihydroxytetrahydrofuran-2-yl)methyl phosphoric) (R)-2-(6-hydroxybenzo[d]thiazol-2-yl)-4,5-dihydrothiazole-4-carboxylic anhydride (LH2-AMP):

This compound was prepared, purified and characterized as reported previously with a few modifications (25, 26). Adenosine-5'-monophosphate (49.5 mg, 0.143 mmol) and D-luciferin (20 mg, 0.071 mmol) were dissolved in DMSO (1 mL), then EDC (274 mg, 1.43 mmol) and DMAP (4.4 mg, 0.036 mmol) in 1 mL DMSO were added and the reaction

mixture was stirred for 15 min at room temperature under argon atmosphere (All reagents and solvents were bubbled with argon before use). The crude product was purified using reversed phase preparative HPLC (conditions described in general methods) and lyophilized to get the pure 6.6 mg of LH2-AMP. LC-MS: rt (min) = 2.46 (4.5 min run).

Acknowledgements. Use of the IMCA-CAT beamline 17-BM at the Advanced Photon Source (APS) was supported by the Industrial Macromolecular Crystallography Association through a contract with the Center for Advanced Radiation Sources at the University of Chicago. Use of the APS was supported by the U. S. DOE, under Contract No. W-31-109-Eng-38.

Douglas S. Auld, Scott Lovell, Natasha Thorne, Wendy A. Lea, David J. Maloney, Min Shen, Ganesha Rai, Kevin Battaile, Craig J. Thomas, Anton Simeonov, Robert P. Hanzlik, and James Inglese, "Molecular Basis for the High Affinity Binding and Stabilization of Firefly Luciferase by PTC124." Proc. Nat. Acad. Sci. USA 2010, 107, 4878-83. PMID 20194791. Publisher's official version: http://dx.doi.org/10.1073/pnas.0909141107

Supplementary Information References:

1. Fraga H, Fernandes D, Fontes R, & Esteves da Silva JC (2005) Coenzyme A affects firefly luciferase luminescence because it acts as a substrate and not as an allosteric effector. *FEBS J* 272(20):5206-5216.
2. Nakatsu T*, et al.* (2006) Structural basis for the spectral difference in luciferase bioluminescence. *Nature* 440(7082):372-376.
3. Conti E, Franks NP, & Brick P (1996) Crystal structure of firefly luciferase throws light on a superfamily of adenylate-forming enzymes. *Structure* 4(3):287-298.
4. Rhodes WC & Mc EW (1958) The synthesis and function of luciferyl-adenylate and oxyluciferyl-adenylate. *J Biol Chem* 233(6):1528-1537.
5. Shrake A & Ross PD (1988) Biphasic denaturation of human albumin due to ligand redistribution during unfolding. *J Biol Chem* 263(30):15392-15399.
6. Celej MS, Montich GG, & Fidelio GD (2003) Protein stability induced by ligand binding correlates with changes in protein flexibility. *Protein Sci* 12(7):1496-1506.
7. Shrake A, Finlayson JS, & Ross PD (1984) Thermal Stability of Human Albumin Measured by Differential Scanning Calorimetry. *Vox Sanguinis* 47(1):7-18.
8. Shrake A & Ross PD (1990) Ligand-induced biphasic protein denaturation. *J Biol Chem* 265(9):5055-5059.
9. Conti E, Lloyd LF, Akins J, Franks NP, & Brick P (1996) Crystallization and preliminary diffraction studies of firefly luciferase from Photinus pyralis. *Acta crystallographica* 52(Pt 4):876-878.

10. Otwinowski Z & Minor W (1997) Processing of X-ray Diffraction Data Collected in Oscillation Mode. In Methods in Enzymology,Macromolecular Crystallography, part A. eds Carter CW & Sweet RM (Academic Press, New York), pp 307-326.
11. Carson M (1997) Ribbons. *Methods Enzymol* 277:493-505.
12. Franks NP, Jenkins A, Conti E, Lieb WR, & Brick P (1998) Structural basis for the inhibition of firefly luciferase by a general anesthetic. *Biophys J* 75(5):2205-2211.
13. A.A.Vagin & A.Teplyakov (1997) *MOLREP*: an Automated Program for Molecular Replacement *J. Appl. Cryst.* 30:1022-1025.
14. Murshudov GN, Vagin AA, & Dodson EJ (1997) Refinement of macromolecular structures by the maximum-likelihood method. *Acta crystallographica* 53(Pt 3):240-255.
15. Emsley P & Cowtan K (2004) Coot: model-building tools for molecular graphics. *Acta crystallographica* 60(Pt 12 Pt 1):2126-2132.
16. Halgren & Thomas S (1996) *J. Comput. Chem* 17:490-519
17. MOE (2008) *MOE Molecular Operating EnVironment* (Chemical Computing Group Inc, Montreal, Canada).
18. Case DA*, et al.* (2002) *Amber 7* (University of California, San Francisco).
19. Niesen FH, Berglund H, & Vedadi M (2007) The use of differential scanning fluorimetry to detect ligand interactions that promote protein stability. *Nat Protoc* 2(9):2212-2221.
20. Almstead NG, Hwang PG, Pines S, Moon Y, & Takasugi JJ (2008).
21. Welch EM*, et al.* (2007) PTC124 targets genetic disorders caused by nonsense mutations. *Nature* 447(7140):87-91.

22. Brown P, *et al.* (1999) Molecular recognition of tyrosinyl adenylate analogues by prokaryotic tyrosyl tRNA synthetases. *Bioorg Med Chem* 7(11):2473-2485.

23. Somu RV, *et al.* (2006) Rationally designed nucleoside antibiotics that inhibit siderophore biosynthesis of Mycobacterium tuberculosis. *J Med Chem* 49(1):31-34.

24. Wang T, *et al.* (2007) Design, synthesis, and molecular modeling studies of 5'-deoxy-5'-ureidoadenosine: 5'-ureido group as multiple hydrogen bonding donor in the active site of S-adenosylhomocysteine hydrolase. *Bioorg Med Chem Lett* 17(16):4456-4459.

25. Goto T & Imai K (1988) Improved Synthesis of Firefly D-Luciferyl-D-adenylate-A Key Intermediate of Firefly Bioluminescence. *Agric. Biol. Chem.* 52(11):2803-2809.

26. Viviani VR & Ohmiya Y (2006) Bovine serum albumin displays luciferase-like activity in presence of luciferyl adenylate: insights on the origin of protoluciferase activity and bioluminescence colours. *Luminescence* 21(4):262-267.

Douglas S. Auld, Scott Lovell, Natasha Thorne, Wendy A. Lea, David J. Maloney, Min Shen, Ganesha Rai, Kevin Battaile, Craig J. Thomas, Anton Simeonov, Robert P. Hanzlik, and James Inglese, "Molecular Basis for the High Affinity Binding and Stabilization of Firefly Luciferase by PTC124." Proc. Nat. Acad. Sci. USA 2010, 107, 4878-83. PMID 20194791. Publisher's official version: http://dx.doi.org/10.1073/pnas.0909141107

Table S1

	Luc:PTC124-AMP (PDB: 3IES)	Luc:Apo (PDB: 3IEP)	Luc:Apo2 (PDB: 3IER)
Data collection			
Space group	$P4_1$	$P4_1$	$P4_1$
Cell dimensions			
a, *b*, *c* (Å)	83.65, 83.65, 97.10	84.69, 84.69, 96.84	84.23, 84.23, 96.91
α, β, γ (°)	90, 90, 90	90, 90, 90	90, 90, 90
Resolution (Å)	50 – 2.0 (2.07-2.0)*	50 – 2.1 (2.18 – 2.1)*	50 – 2.05 (2.12 – 2.05)*
R_{sym} or R_{merge}	0.107 (0.494)	0.132 (0.518)	0.123 (0.479)
$I / \sigma I$	12.6 (2.3)	11.3 (2.7)	11.1 (2.2)
Completeness (%)	98.8 (97.3)	99.9 (100.0)	99.6 (98.7)
Redundancy	5.0 (4.6)	5.1 (5.0)	4.9 (4.2)
Refinement			
Resolution (Å)	50 – 2.0	50 – 2.1	50 – 2.05
No. reflections	42,282	37,872	39,997
R_{work} / R_{free}	0.182 / 0.218	0.188 / 0.221	0.183 / 0.225
No. atoms			
Protein	3,384	3,353	3,360
Ligand/ion	43		10
Water	234	199	197
B-factors (Å^2)			
Protein	22.9	30.8	23.6
Ligand/ion	22.0		39.6
Water	31.4	36.9	29.6
R.m.s. deviations			
Bond lengths (Å)	0.013	0.018	0.023
Bond angles (°)	1.430	1.603	1.926

*Values in parentheses are for highest-resolution shell.

Douglas S. Auld, Scott Lovell, Natasha Thorne, Wendy A. Lea, David J. Maloney, Min Shen, Ganesha Rai, Kevin Battaile, Craig J. Thomas, Anton Simeonov, Robert P. Hanzlik, and James Inglese, "Molecular Basis for the High Affinity Binding and Stabilization of Firefly Luciferase by PTC124." Proc. Nat. Acad. Sci. USA 2010, 107, 4878-83. PMID 20194791. Publisher's official version: http://dx.doi.org/10.1073/pnas.0909141107

Table S2

R1	R2		FLuc (μM)	FLuc + CoASH (μM)	FLuc + Cys (μM)
o-F	*m*-COOH	**(1)**	0.014 ± 0.008	0.32 ± 0.21	0.0082 ± 0.003
o-F	*p*-COOH	**(7)**	0.72 ± 0.45	6.2 ± 1.1	0.36 ± 0.25
o-F	*m*-CONH (sa-Ade)	**(12)**	0.005 ± 0.001	0.003 ± 0.001	N/D
o-F	*p*-CONH (sa-Ade)	**(13)**	0.003 ± 0.001	0.003 ± 0.001	N/D

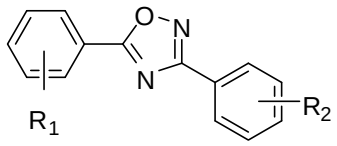

Figure S1

Douglas S. Auld, Scott Lovell, Natasha Thorne, Wendy A. Lea, David J. Maloney, Min Shen, Ganesha Rai, Kevin Battaile, Craig J. Thomas, Anton Simeonov, Robert P. Hanzlik, and James Inglese, "Molecular Basis for the High Affinity Binding and Stabilization of Firefly Luciferase by PTC124." Proc. Nat. Acad. Sci. USA 2010, 107, 4878-83. PMID 20194791. Publisher's official version: http://dx.doi.org/10.1073/pnas.0909141107

A

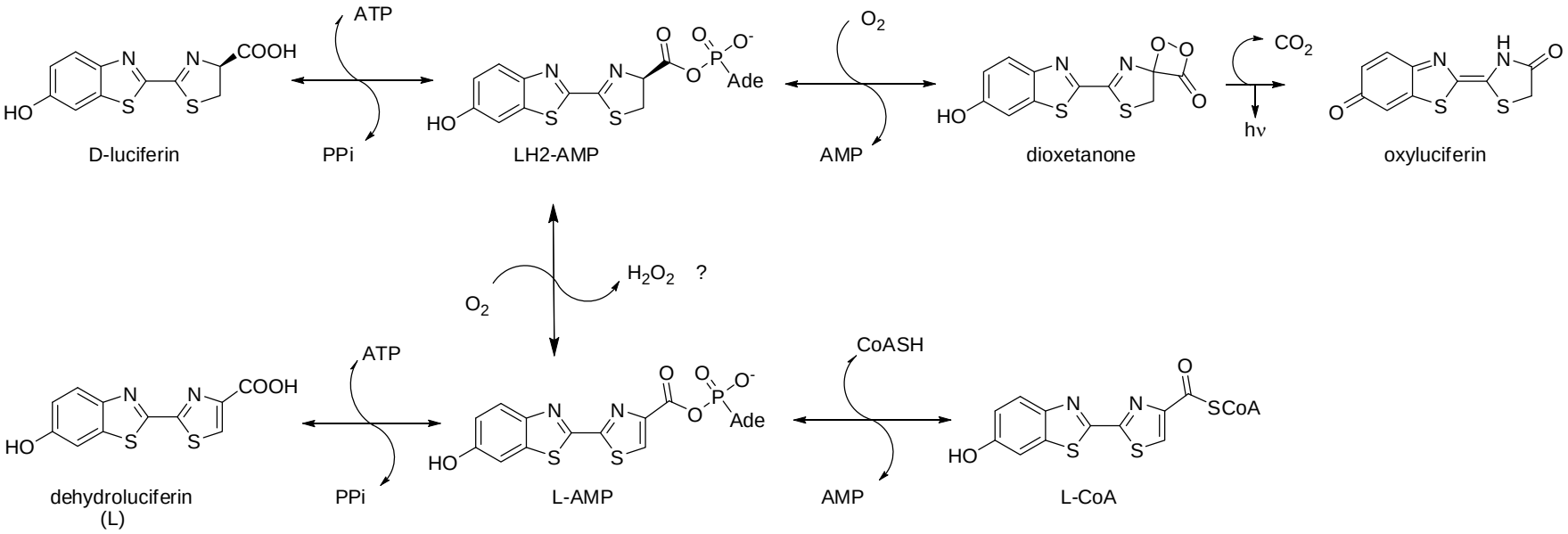

B

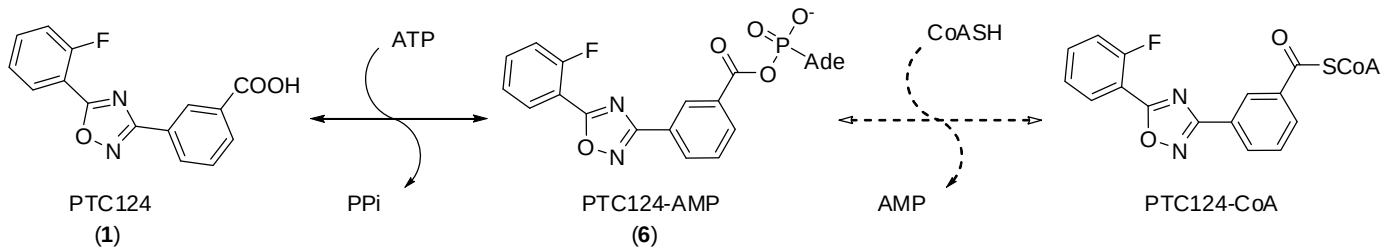

Figure S2

Douglas S. Auld, Scott Lovell, Natasha Thorne, Wendy A. Lea, David J. Maloney, Min Shen, Ganesha Rai, Kevin Battaile, Craig J. Thomas, Anton Simeonov, Robert P. Hanzlik, and James Inglese, "Molecular Basis for the High Affinity Binding and Stabilization of Firefly Luciferase by PTC124." Proc. Nat. Acad. Sci. USA 2010, 107, 4878-83. PMID 20194791. Publisher's official version: http://dx.doi.org/10.1073/pnas.0909141107

A

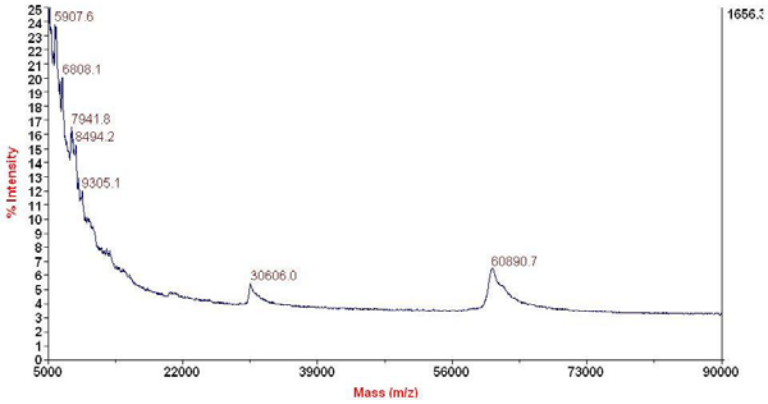

B

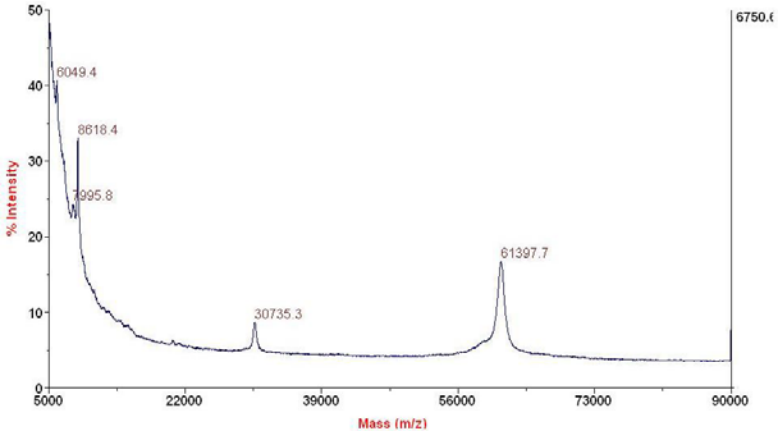

Figure S3A

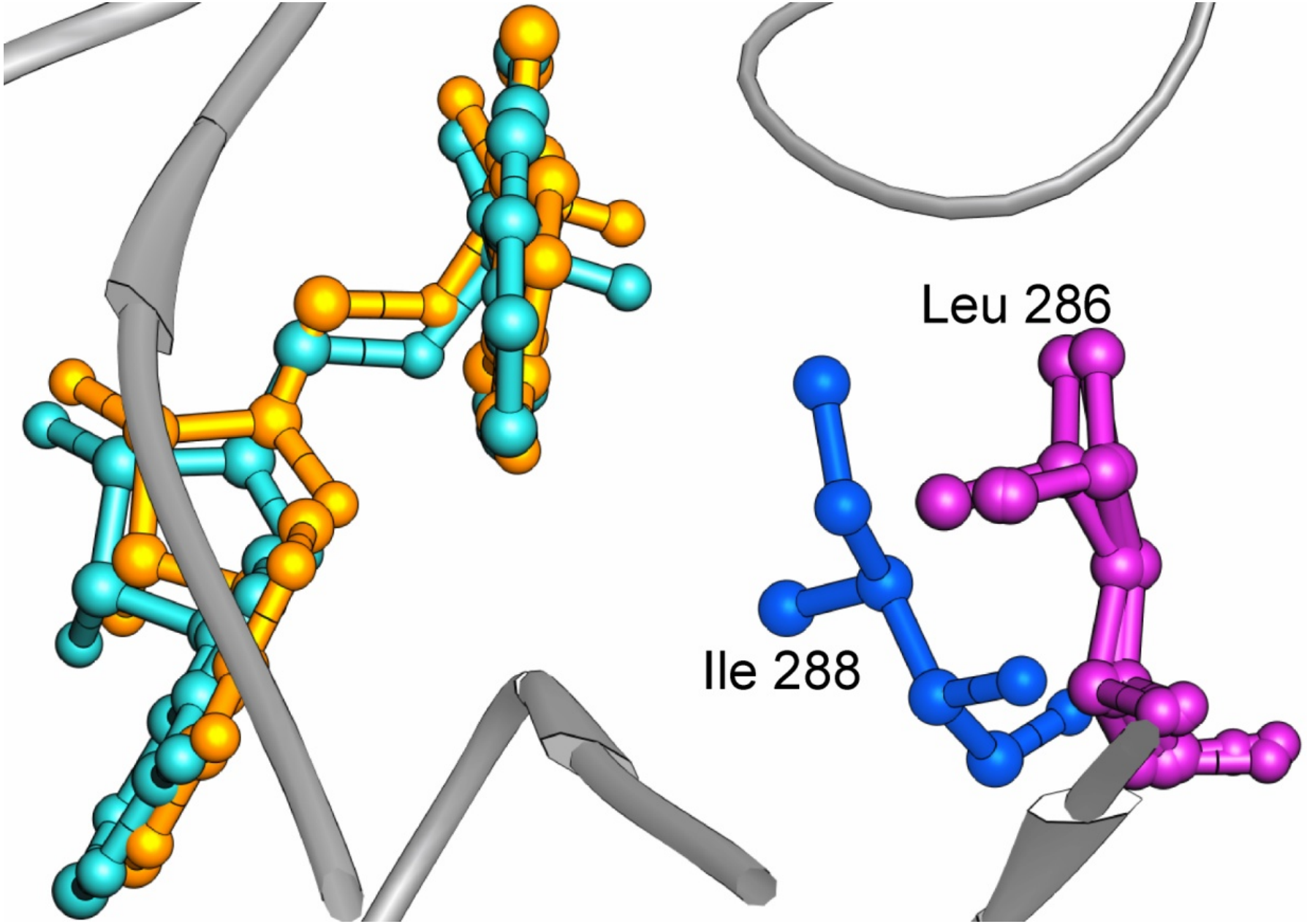

Figure S3B

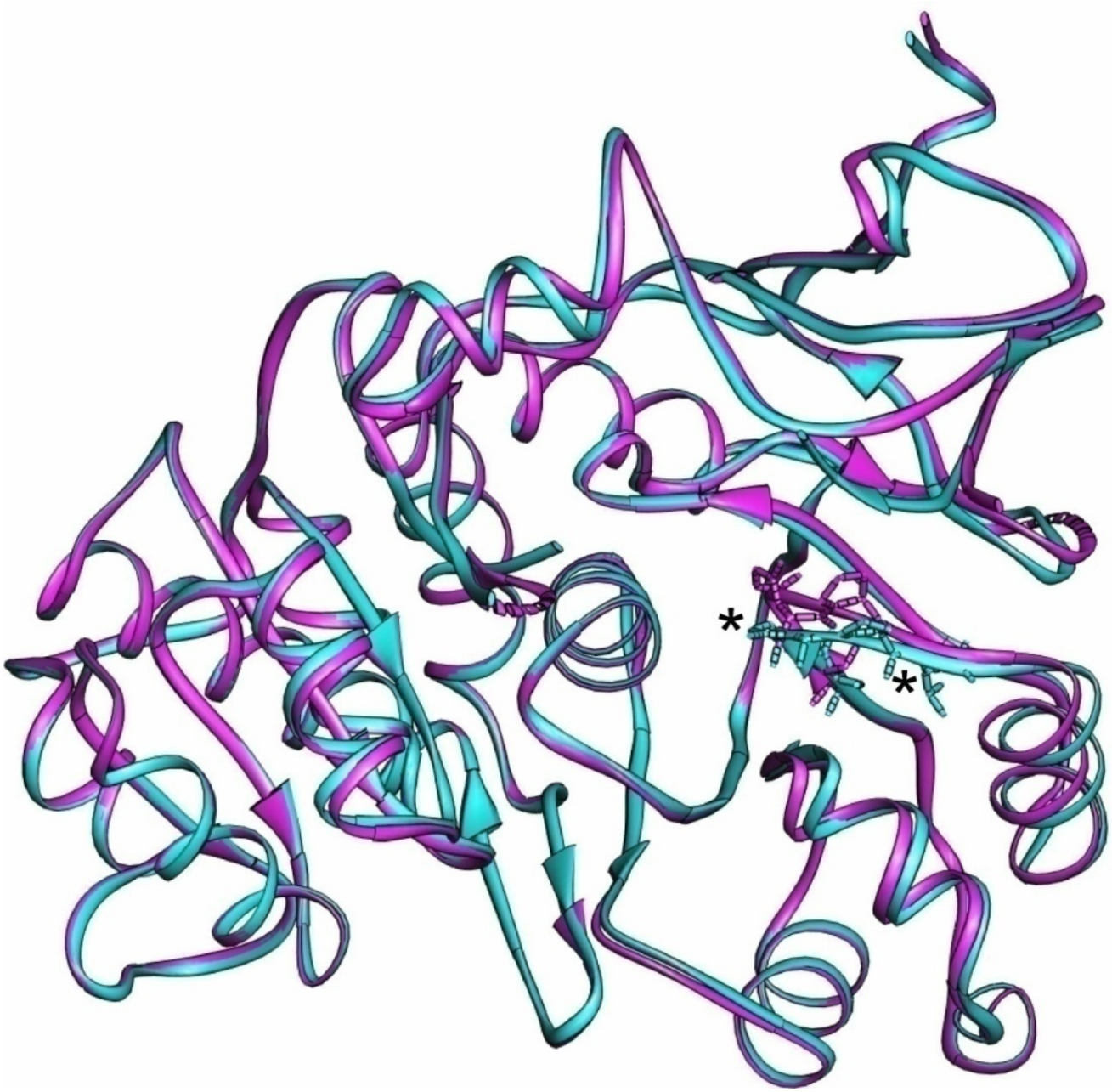

Figure S3C

i

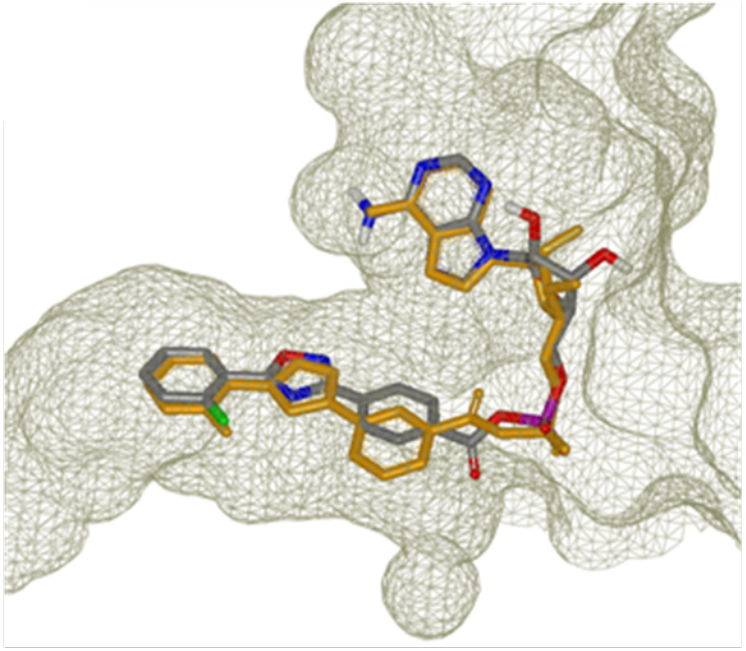

ii

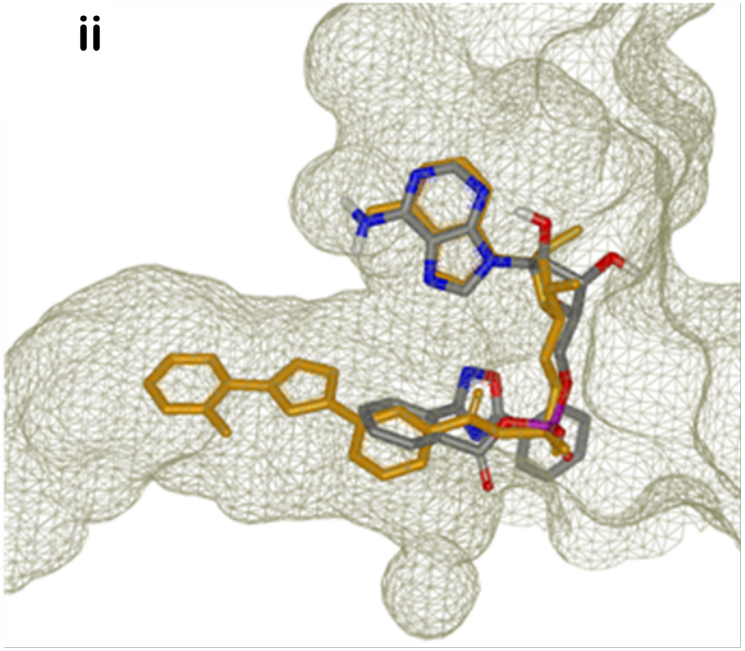

iii

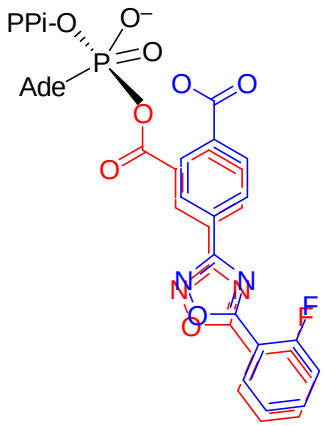

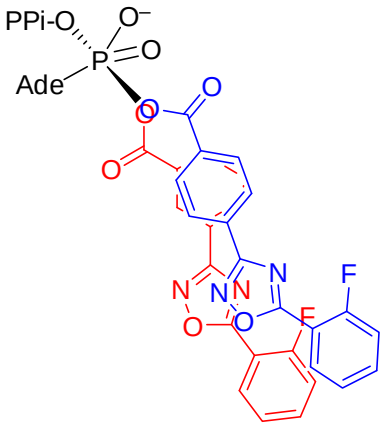

Figure S4

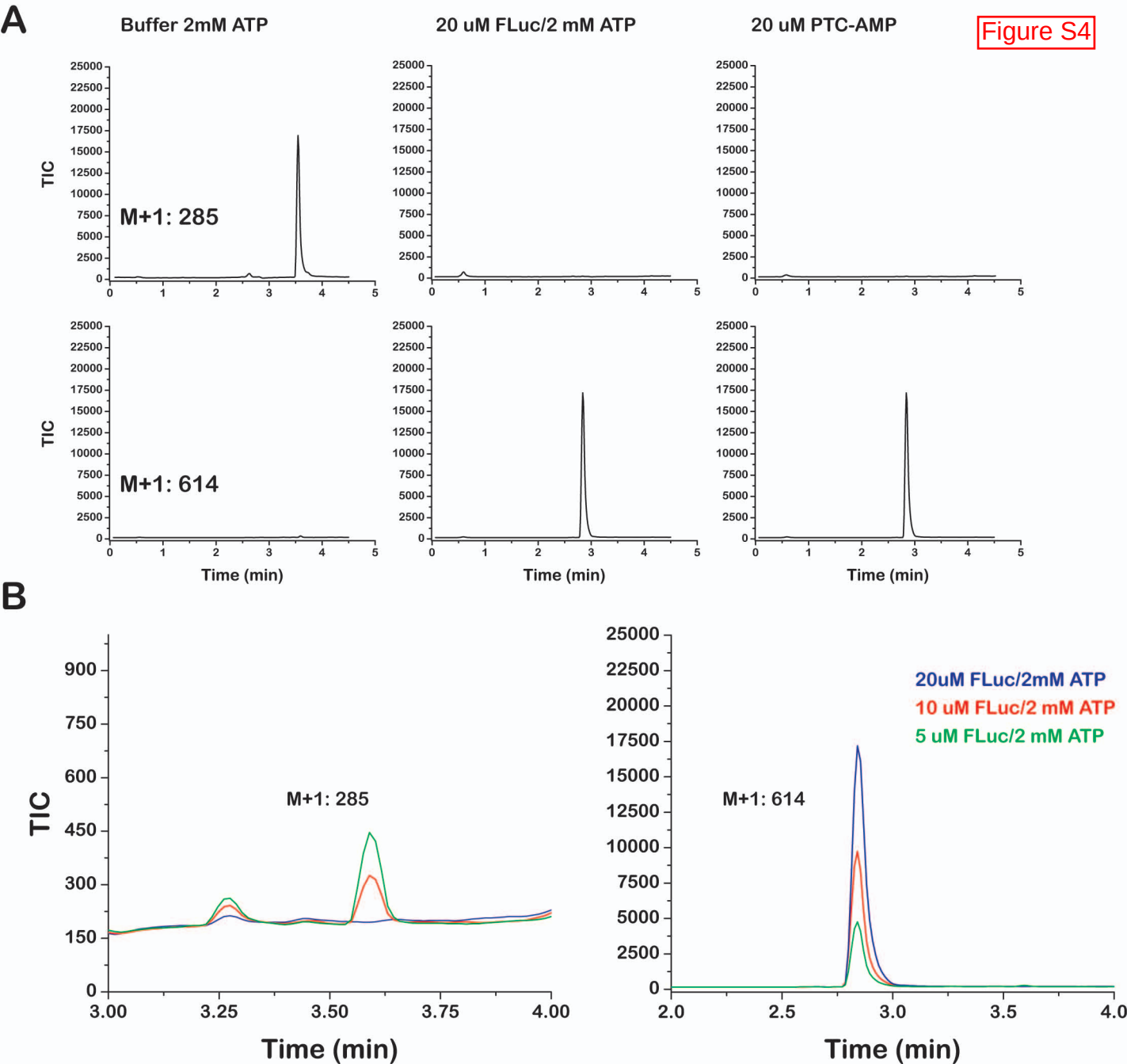
A
Buffer 2mM ATP
20 uM FLuc/2 mM ATP
20 uM PTC-AMP
TIC
M+1: 285
M+1: 614
Time (min)
B
TIC
M+1: 285
M+1: 614
20uM FLuc/2mM ATP
10 uM FLuc/2 mM ATP
5 uM FLuc/2 mM ATP
Time (min)

Figure S5

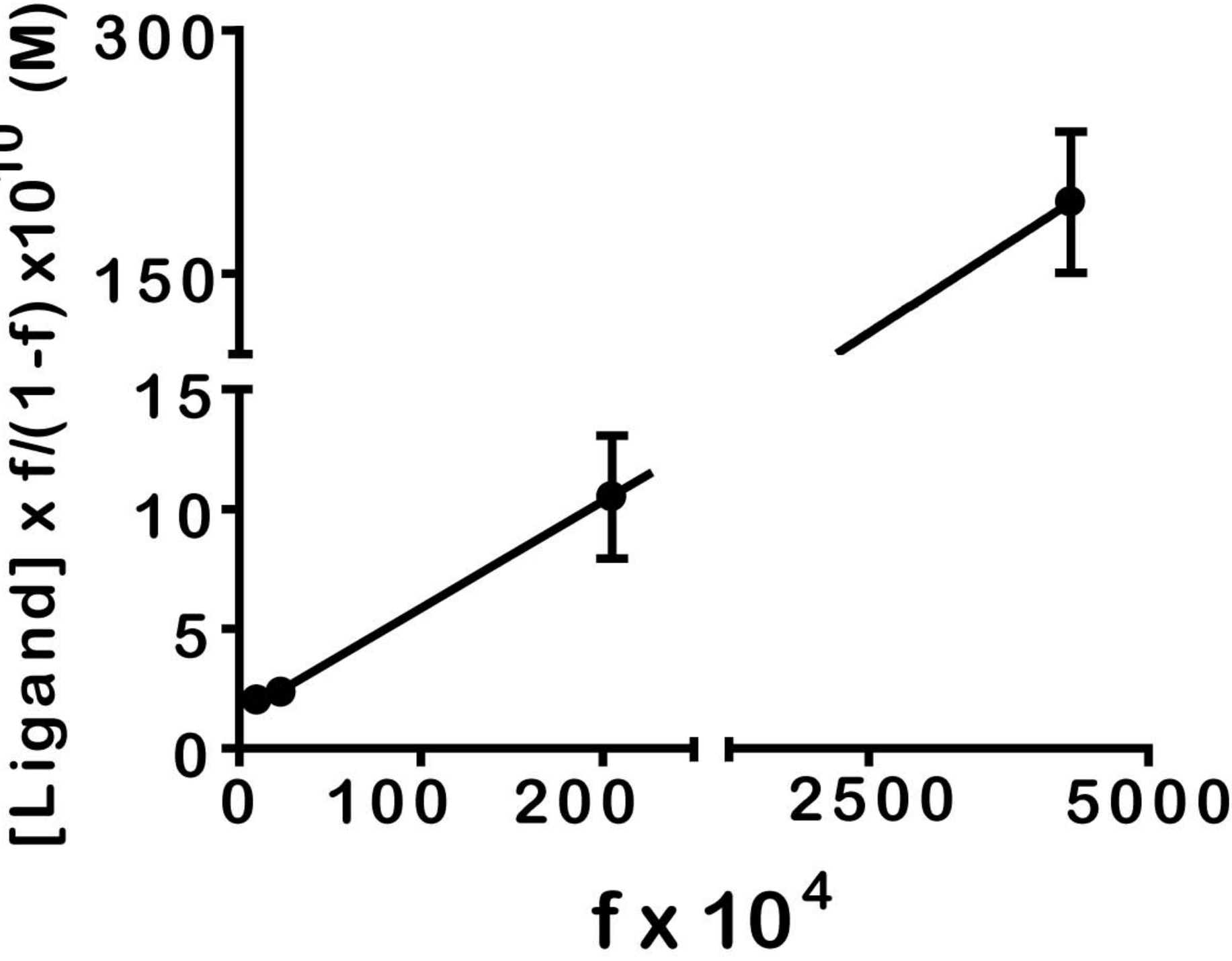

Figure S6

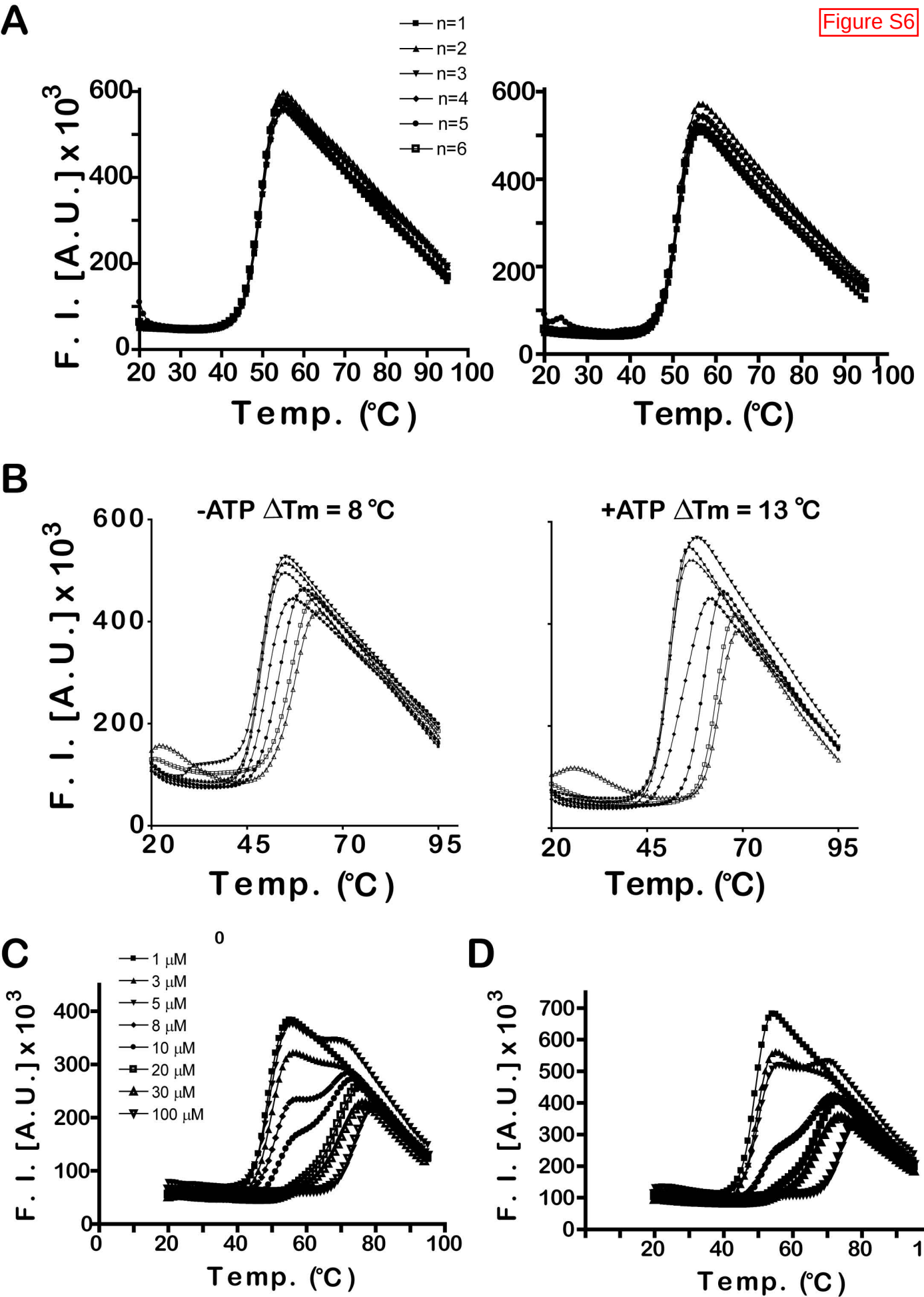
A
n=1
n=2
n=3
n=4
n=5
n=6
F. I. [A.U.] x 10^3
600
400
200
0
20 30 40 50 60 70 80 90 100
Temp. (°C)
B
-ATP ΔTm = 8 °C
+ATP ΔTm = 13 °C
20 45 70 95
C
0
1 μM
3 μM
5 μM
8 μM
10 μM
20 μM
30 μM
100 μM
0 20 40 60 80 100
D
700
600
500

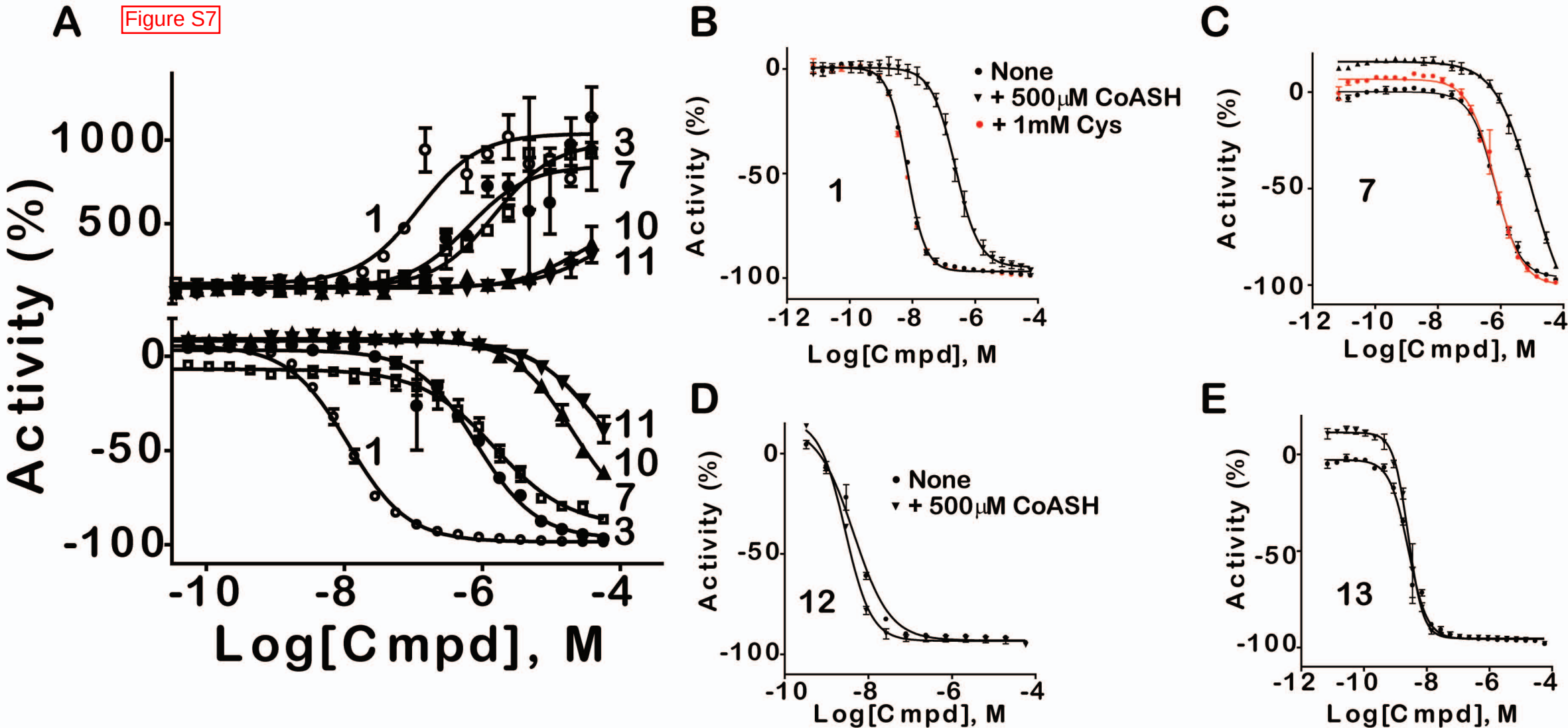
A
Figure S7
Activity (%)
Log[Cmpd], M
1
3
7
10
11
B
None
+ 500μM CoASH
+ 1mM Cys
C
D
E
12
13